Redox Biology 60 (2023) 102614

Contents lists available at ScienceDirect

Redox Biology

journal homepage: www.elsevier.com/locate/redox

# GAT107-mediated α7 nicotinic acetylcholine receptor signaling attenuates inflammatory lung injury and mortality in a mouse model of ventilator-associated pneumonia by alleviating macrophage mitochondrial oxidative stress via reducing MnSOD-S-glutathionylation

Alex G. Gauthier [a], Mosi Lin [a], Sidorela Zefi [a], Abhijit Kulkarni [c], Ganesh A. Thakur [c], Charles R. Ashby Jr. [a], Lin L. Mantell [a,b,*]

[a] Department of Pharmaceutical Sciences, College of Pharmacy and Health Sciences, St. John's University, Queens, NY, USA
[b] Feinstein Institute for Medical Research, Northwell Health, Manhasset, NY, USA
[c] Northeastern University, Boston, MA, USA

ARTICLE INFO

*Keywords:*
Survival
α7nAChR
HMGB1
Inflammatory lung injury
Mitochondria
MnSOD glutathionylation

ABSTRACT

Supraphysiological concentrations of oxygen (hyperoxia) can compromise host defense and increase susceptibility to bacterial and viral infections, causing ventilator-associated pneumonia (VAP). Compromised host defense and inflammatory lung injury are mediated, in part, by high extracellular concentrations of HMGB1, which can be decreased by GTS-21, a partial agonist of α7 nicotinic acetylcholine receptor (α7nAChR). Here, we report that a novel α7nAChR agonistic positive allosteric modulator (ago-PAM), GAT107, at 3.3 mg/kg, i.p., significantly decreased animal mortality and markers of inflammatory injury in mice exposed to hyperoxia and subsequently infected with *Pseudomonas aeruginosa*. The incubation of macrophages with 3.3 μM of GAT107 significantly decreased hyperoxia-induced extracellular HMGB1 accumulation and HMGB1-induced macrophage phagocytic dysfunction. Hyperoxia-compromised macrophage function was correlated with impaired mitochondrial membrane integrity, increased superoxide levels, and decreased manganese superoxide dismutase (MnSOD) activity. This compromised MnSOD activity is due to a significant increase in its level of glutathionylation. The incubation of hyperoxic macrophages with 3.3 μM of GAT107 significantly decreases the levels of glutathionylated MnSOD, and restores MnSOD activity and mitochondrial membrane integrity. Thus, GAT107 restored hyperoxia-compromised phagocytic functions by decreasing HMGB1 release, most likely via a mitochondrial-directed pathway. Overall, our results suggest that GAT107 may be a potential treatment to decrease acute inflammatory lung injury by increasing host defense in patients with VAP.

## 1. Introduction

Patients in intensive care units (ICUs) are often given supplemental oxygen therapy up to 100% oxygen (hyperoxia, >21% oxygen) [1–3]. Although oxygen therapy is a lifesaving intervention, prolonged exposure to hyperoxia can produce acute inflammatory lung injury and compromise lung host defense [2,4–6]. Consequently, compromised host defense can contribute to an increased susceptibility to pulmonary bacterial infections that cause ventilator-associated pneumonia (VAP) in patients receiving oxygen therapy, especially those receiving mechanical ventilation [7,8].

Alveolar macrophages are the first line of defense against invading pathogens that enter the distal airways [9–11]. In *ex vivo* cultures of alveolar macrophages, prolonged exposure to hyperoxia impairs the phagocytosis of bacteria known to produce VAP, such as *Staphylococcus aureus*, *Pseudomonas aeruginosa* (PA), and bacteria from the *Enterobacteriaceae* family [7,12,13]. Since alveolar macrophages in the airways are essential against invading pathogens, impairment of their functions can increase the susceptibility to bacterial infections in patients receiving oxygen therapy and animals exposed to hyperoxia [14–17].

It has been reported that VAP patients had a 17-fold higher level of high mobility group box-1 (HMGB1) protein in their airways, compared

* Corresponding author. Department of Pharmaceutical Sciences, St. John's University College of Pharmacy and Health Sciences, 128 St. Albert Hall, 8000 Utopia Parkway, Queens, NY, 11439, USA.
*E-mail addresses:* mantelll@stjohns.edu, lmantell@northwell.edu (L.L. Mantell).

https://doi.org/10.1016/j.redox.2023.102614
Received 5 November 2022; Received in revised form 9 January 2023; Accepted 18 January 2023
Available online 20 January 2023

to healthy controls [18]. HMGB1 is a nuclear protein that can be secreted from immune cells, such as alveolar macrophages, into the extracellular milieu, where it functions as a late mediator of inflammation [19,63]. The high levels of accumulated extracellular airway HMGB1 play a major role in the compromised host defense against bacterial infection in both mice with cystic fibrosis and those subjected to hyperoxia [15,21]. Therefore, decreasing the extracellular levels of HMGB1 could represent a therapeutic approach for the treatment of VAP.

The activation of α7 nicotinic acetylcholine receptors (α7nAChRs) in alveolar macrophages, with the partial-agonist, GTS-21, significantly decreases the active release and extracellular accumulation of HMGB1 [17]. The α7nAChR is a homomeric pentamer that is a ligand-gated ion channel on neuronal and non-neuronal cells [22–24]. *In vitro,* GTS-21 significantly decreases the active release and extracellular accumulation of HMGB1 [17]. In addition, the active release of HMGB1 from hyperoxia-compromised macrophages results from the activation of NF-κB and the subsequent hyper-acetylation of lysine residues on HMGB1 is required for its translocation from the nucleus to the cytoplasm. Interestingly, although GTS-21 significantly increased bacterial clearance and decreased lung injury in hyperoxia-exposed mice with *P. aeruginosa* pneumonia [17], GTS-21 did not significantly alter the mortality rate (data not shown). Consequently, we wanted to determine the efficacy of a next generation α7nAChR activator on animal survival in a mouse model of VAP and the potential mechanisms in an *in vitro* model, where macrophage functions are compromised by exposure to hyperoxia.

GAT107, a (+)-enantiomer of racemic 4-(4-bromophenyl)-3a,4,5,9b-tetrahydro-3H-cyclopenta[*c*]quinoline-8-sulfonamide, is a positive allosteric modulator (PAM) and direct allosteric activator (DAA) that 1) increases or potentiates the response to orthosteric site ligands and 2) activates the α7nAChR ion channel (in the absence of an orthosteric agonist) by binding to an allosteric site distinct from that of the PAM site [25–27]. Interestingly, *in vitro*, the α7nAChR can be rapidly desensitized by acetylcholine (ACh) and the co-administration of GAT107 with ACh produces a significant decrease in the ACh-induced desensitization [25–27]. It is likely that GAT107 facilitates the conversion from desensitized states to conducting states which surmounts receptor desensitization [25–27].

In a previous study, we reported that GAT107 was efficacious in restoring hyperoxia-compromised macrophage bacterial phagocytosis in cultured cells and bacterial clearance from the airways in mice exposed to hyperoxia that were subsequently exposed to PA via intratracheal administration [28]. In this study, we further determined whether GAT107 can significantly increase the survival rate in a mouse model of VAP. In this study, we report that GAT107 significantly increased the probability of survival and decreased hyperoxia-induced acute inflammatory lung injury by decreasing hyperoxia-induced NF-κB activation and decreasing HMGB1 release from macrophages into the airways. The prolonged exposure of macrophages to hyperoxia induces oxidative stress and mitochondrial damage [29–31]. Our results indicated that hyperoxia-induced mitochondrial damage is correlated with *S*-glutathionylation of manganese superoxide dismutase (MnSOD), and this is significantly decreased by GAT107.

## 2. Materials and methods

### 2.1. Animal studies

Male C57BL/6 mice (6–10 weeks old; The Jackson Laboratory, Bar Harbor, ME, USA) were used in this investigation, based on a protocol (protocol #1953) approved by the Institutional Animal Care and Use Committees of St. John's University. The mice were housed in a specific pathogen-free environment, maintained at 22 °C in ≈50% relative humidity and a 12 h light/dark cycle. All mice had *ad libitum* access to standard rodent food and water. Mice were randomized to receive either 3.3 mg/kg of GAT107 ((+)-(4-(4-bromophenyl)-3a,4,5,9b-tetrahydro-3H-cyclopenta[*c*]quinoline-8-sulfonamide), donated by Dr. Ganesh A. Thakur (Northeastern University, Boston, MA) or vehicle control (DMSO), administered by intraperitoneal injection, every 12 h, starting 24 h after the onset of hyperoxic exposure until the termination of hyperoxia exposure. After 48 h of exposure, the mice were inoculated with $0.1 \times 10^8$ colony-forming units (CFUs) of *Pseudomonas aeruginosa* (PA) through a 1- to 2-cm incision on the neck to expose the trachea after anesthetization with sodium pentobarbital (75 mg/kg i.p.). We selected PAO1, a laboratory strain of PA, as the pathogen to induce lung infection as it has been reported to account for 21% of all VAP cases [32], as described in our published studies [15]. Twenty-four hours after bacterial inoculation, mice were euthanized, and bronchoalveolar lavage (BAL) fluid was collected and analyzed for markers of lung injury and inflammatory responses. For animal survival studies, mice were subjected to hyperoxia exposure for 72 h and inoculated similarly as stated above and as described [15,21,33]. Mice were then monitored every hour over the course of 24 h for survival.

### 2.2. Exposure to hyperoxia

Male C57BL/6 mice were placed in microisolator cages (Allentown Caging Equipment, Allentown, NJ, USA), which were kept in a Plexiglas chamber (BioSpherix, Lacona, NY, USA) and exposed to ≥ 95% $O_2$ for up to 72 h. The exposure of murine macrophage RAW 264.7 cells was conducted in humidified Plexiglas chambers (Billups-Rothenberg, Del Mar, CA, USA), flushed with 95% $O_2$/5% $CO_2$, at 37 °C for 24 h. An oxygen analyzer (MSA; Ohio Medical Corporation, Gurnee, IL, USA) was used to monitor the oxygen concentration in the chamber.

### 2.3. Bronchoalveolar lavage (BAL) and protein quantification

Mice were anesthetized using sodium pentobarbital (120 mg/kg i.p.). A 1- to 2-cm incision was made on the neck, the trachea was dissected, and a 20-gauge × 1.25-inch intravenous catheter was inserted caudally into the lumen of the exposed trachea. The lungs were gently lavaged twice with 1 mL of sterile, nonpyrogenic phosphate-buffered saline (PBS) solution (Mediatech, Herndon, VA, USA) containing a cocktail of protease and phosphatase inhibitors (Thermo Fisher, Waltham, MA). BAL samples were centrifuged at 200×*g* at 4 °C for 5 min, and the resultant supernatants were stored flash frozen in liquid nitrogen and then stored in a freezer at −80 °C. Total protein content in the BAL was determined using the Pierce Bicinchoninic acid (BCA) assay Kit (Thermo Fisher, Waltham, MA), as per the manufacturer's instructions.

### 2.4. Differential cell counting

Mouse BAL samples were obtained as described above. BAL samples were centrifuged at 200×*g* at 4 °C for 5 min, and the pellet was obtained and resuspended in red blood cell lysis buffer. Subsequently, total leukocyte counts were determined using a hemocytometer and an equal quantity of total leukocytes per sample was mounted onto slides using a Shandon Cytospin Centrifuge. The slides were then stained with hematoxylin and eosin and neutrophils were identified and counted manually using a hemocytometer, as described previously [17].

### 2.5. Cell culture and special reagents

Murine macrophage-like RAW 264.7 cells (TIB-71; American Type Culture Collection (ATCC), Manassas, VA) were cultured in Dulbecco's Modified Eagle Medium (DMEM) and supplemented with 10% Fetal Bovine Serum (Atlanta Biologicals, Lawrenceville, GA). Cells were maintained at 37 °C in normoxia (5% $CO_2$/21% $O_2$) for 24 h, allowed to grow to 70–80% confluency, and subcultured every 2 days.

### 2.6. Phagocytosis assay

RAW 264.7 cells were seeded in 24-well plates, allowed to adhere for 6 h, and then exposed to 10 μg/mL of recombinant HMGB1 (rHMGB1) (donated by Dr. Haichao Wang of the Feinstein Institutes for Medical Research, Manhasset, NY, USA), which was administered simultaneously with GAT107 or the vehicle control. RAW 264.7 cells were incubated at 37 °C for 1 h with opsonized fluorescein isothiocyanate (FITC)-labeled latex beads (Polysciences, Warrington, PA), at a ratio of 100 : 1 (beads: cell). Macrophages were incubated with 0.04% Trypan blue in PBS for 10 min to quench beads that were not internalized by macrophages. To visualize the uptake of FITC-labeled latex beads, macrophages were fixed with 4% paraformaldehyde for 10 min, washed once with PBS, and stained with 4′,6-diamidino-2-phenylindole (DAPI) (Molecular Probes, Eugene, OR). To visualize the cell cytoskeleton, cells were stained with rhodamine phalloidin (Molecular Probes, Eugene, OR). The phagocytosis or uptake of the beads was assessed visually using an Evos Fluorescent Microscope (Thermo Fischer, Waltham, MA) and 200 individual macrophages per well in duplicates from three independent experiments were allocated for each experimental group as described [17].

### 2.7. Western blot analysis and p65 binding activity

The levels of extracellular HMGB1 were determined in RAW 264.7 macrophages cultured in serum-free Opti-MEM I medium (Gibco, Waltham, MA), and RAW cells were cultured in DMEM with 10% FBS for analysis of intracellular proteins, such as actin. Macrophages were seeded in 6-well plates and exposed to hyperoxia and incubated with GAT107 as described above. For the analysis of extracellular HMGB1 in the cell culture media, after hyperoxic exposure, the cell culture supernatant was collected and centrifuged at 130×*g* at 4 °C for 10 min and concentrated using 10 kDa Centricon centrifugal filter (Millipore Sigma, Burlington, MA). For intracellular protein analysis, cells were washed three times in PBS and lysed with a cell lysis buffer (Cell Signaling Technology, Danvers, MA) that contained a protease and phosphatase inhibitor cocktail (Thermo Fischer, Waltham, MA). The total protein content of cell lysate was determined using the Pierce Bicinchoninic acid (BCA) assay Kit (Thermo Fisher, Waltham, MA), as per the manufacturer's instructions. Samples were loaded onto 12% or 15% SDS–polyacrylamide gels (Bio-Rad, Hercules, CA) and transferred to Immobilon-P membranes (Millipore, Bedford, MA). Nonspecific binding sites on the membrane were blocked by incubating the membrane with 5% nonfat dry milk (Bio-Rad, Hercules, CA) in Tris-buffered saline (TBS), containing 0.1% Tween 20 (TBST), for 1 h at room temperature. Subsequently, the membranes were washed three times with TBST and incubated overnight at 4 °C with *anti*-HMGB1 antibody (1:1000, #6893, Cell Signaling), *anti*-MnSOD antibody (1:1000, #AD-SOD-110, Enzo, New York, NY), and anti-pan-actin antibody (1:1000, #8456, Cell Signaling), diluted in 5% nonfat dry milk in TBST. After three washes with TBST, the membranes were incubated with goat anti-rabbit horseradish peroxides–coupled secondary antibody (1:5000; GE Healthcare, Chicago, IL) for 1 h at room temperature. Subsequently, membranes were washed three times with TBST, and the immunoreactive proteins were visualized using the SuperSignal West Pico Plus Chemiluminescent Substrate (Thermo Fisher, Waltham, MA) per the manufacturer's instructions. The images were developed using a Bio-Rad ChemiDoc XRS imaging system (Bio-Rad, Hercules, CA). Immunoreactive bands were quantified using ImageJ software (version 2.0.0).

Western blot assays were used to determine the level of NF-κB (p65) in cell lysates, using a Transcription Factor Assay Kit (Cayman Chemical, Ann Harbor, MI). The amount of transcriptionally active and free unbound NF-κB subunit p65 was measured based on its interaction with a double-stranded specific DNA sequence, using an enzyme-linked immunosorbent assay. A colorimetric product was formed and measured spectrophotometrically at 450 nm, using a Synergy LX multimode reader (Biotek, Winooski, VT, USA). Data was compared to a standard curve and normalized to total protein content.

### 2.8. Measurement of mitochondrial membrane potential and mitochondrial superoxide

RAW 264.7 cells were seeded in 96-well black wall, clear bottom plates, exposed to hyperoxia, and incubated as described above. Macrophage mitochondrial membrane potential was determined using the tetramethylrhodamine ethyl ester (TMRE) with the Mitochondrial Membrane Potential Assay Kit (Abcam, Cambridge, UK), as per the manufacturer's instructions. In brief, following a 24 h incubation period, cells were incubated with 1 μM of TMRE for 20 min at 37 °C. Prior to TMRE, a negative control for mitochondrial membrane polarization, was generated by incubating the cells with 20 μM of carbonyl cyanide 4-(trifluoromethoxy)phenylhydrazone (FCCP), an uncoupling compound, for 15 min at 37 °C. After incubation with TMRE, the cells were gently washed with PBS containing 0.2% BSA and the level of fluorescence was determined at an excitation wavelength of 549 nm and an emission wavelength of 570 nm, using a Synergy LX multimode reader. The same experimental design was used in another set of experiments that incubated RAW 264.7 cells with Mitotracker Green, as a control, per the manufacturer's protocol (Thermo Fisher, Waltham, MA). The amount of TMRE signal in each condition was normalized to its Mitotracker Green signal and reported as a percent compared to the control. For the measurement of mitochondrial superoxide levels, after 24 h of incubation, macrophages were incubated with 5 μM of the MitoSOX reagent (Invitrogen, Carlsbad, CA), to measure reactive oxygen species (ROS) in mitochondria, for 10 min at 37 °C and washed three times with warm PBS as per the manufacturer's instructions. The presence of mitochondrial superoxide was detected using a Synergy LX multimode reader at excitation and emission wavelengths of 510 and 580 nm, respectively.

### 2.9. Determination of TNFα levels

For detection of TNFα in the cell culture media, samples were prepared as described above for HMGB1 in the western blot assays. Equal volumes of cell culture media were incubated with a commercially available TNFα ELISA (Thermo Fisher, Hampton, NH), as described by the manufacturer's instructions. A colorimetric product was formed and measured spectrophotometrically at 450 nm using a Synergy LX multimode reader (Biotek, Winooski, VT, USA).

### 2.10. Measurement of manganese superoxide dismutase (MnSOD) activity

After 24 h of hyperoxic exposure and incubation with DMSO vehicle control or with 3.3 μM of GAT107, which was administered simultaneously with hyperoxic exposure, RAW 264.7 macrophage cell lysate was prepared as described above. Equal amounts of protein were used and evaluated MnSOD activity, using a superoxide dismutase (SOD) colorimetric activity kit (Thermo Fisher), as per manufacturer's instructions. Non-mitochondrial iron SOD (FeSOD) and copper zinc SOD (CuZnSOD) was inhibited by incubating the cell lysate with cyanide. Cell lysate containing cyanide was then incubated with xanthine oxidase, an enzyme that produces superoxide in the presence of oxygen. The amount of superoxide not dismutated to hydrogen peroxide by MnSOD reacted with a nitro blue tetrazolium reagent to yield a yellow color. This colorimetric product was read at 450 nm, using a Synergy LX multimode reader. The results were compared to a standard curve generated by using bovine erythrocyte SOD (produced without the addition of cyanide) and normalized to total protein concentrations.

### 2.11. Immunoprecipitation and immunodetection

RAW 264.7 cells were exposed to 24 h of hyperoxia and incubated

simultaneously with GAT107 (0 or 3.3 μM) as described above. Cell lysate was collected, and protein content was determined as described for the western blot assay. MnSOD was co-immunoprecipitated from cell lysate using the Pierce Direct Magnetic IP/Co-Immunoprecipitation Kit (Thermo Scientific, Waltham, MA) containing a polyclonal *anti*-MnSOD antibody (Enzo, New York, NY), based on the manufacturer's instructions. After immunoprecipitation, samples were immediately subjected to SDS-PAGE and western blot analysis as described above. Western blot analysis was conducted as described above, using *anti*-MnSOD antibody (1:1000, Enzo, New York, NY) and monoclonal anti-glutathione antibody (1:1000, ViroGen, Watertown, MA).

### 2.12. Statistical analysis

The statistical analyses were done using GraphPad Prism statistical software (version 7.0a). The results are presented as the mean ± SEM. All data sets were analyzed for statistical significance using an analysis of variance (ANOVA) with Dunnett's post hoc analysis. Animal mortality data were analyzed using a Kaplan-Meier curve. Correlation analysis was done using a two-tail Pearson Correlation Coefficient test. A 95% confidence interval was used and a p value less than 0.05 was considered significant.

## 3. Results

### 3.1. Survival studies

Prolonged exposure to hyperoxia is a critical mediator for the increased rates of mortality in patients with pulmonary infection [13,15,34,35,63]. To ascertain whether GAT107 administration to hyperoxia-compromised mice with PA lung infection could increase the survival rate, mice were initially exposed to 72 h of 95% $O_2$. During the 72 h of hyperoxia exposure, mice were given 3.3 mg/kg i.p. of GAT107, based on the previous studies [28,36] or vehicle (DMSO), starting after 24 h of hyperoxia. As previously reported [15] and in Fig. 1, the mice that remained in hyperoxia (>95% $O_2$) had significantly higher mortality rates (20% survival rate, $p < 0.05$), 24 h after exposure to PA intratracheally, compared to mice that remained in room air (21% $O_2$) (100% survival rate). In hyperoxic mice given 3.3 mg/kg i.p. of GAT107 and exposed to PA, there was a significant increase in the survival rate (60% of the mice survived, $p < 0.05$), compared to mice given the vehicle. In addition, GAT107 significantly increased the mean survival time to 18.25 versus 15.25 h in mice given the vehicle. Overall, these data suggest that GAT107 increases the probability of mice surviving following exposure to hyperoxia and intratracheal exposure to PA.

### 3.2. Systemic administration of GAT107 decreases acute inflammatory lung injury

To determine if GAT107-mediated increase in animal survival was due to a decrease in acute inflammatory lung injury, mice were exposed to 48 h of 95% $O_2$ prior to PA inoculation, as described previously [15]. During the 48 h of hyperoxia exposure, mice were given 3.3 mg/kg i.p. of GAT107 or vehicle (DMSO). After 48 h, mice were intratracheally inoculated with PA, which produced pulmonary infection and inflammation. Twenty-four hours after intratracheal inoculation, the BAL was

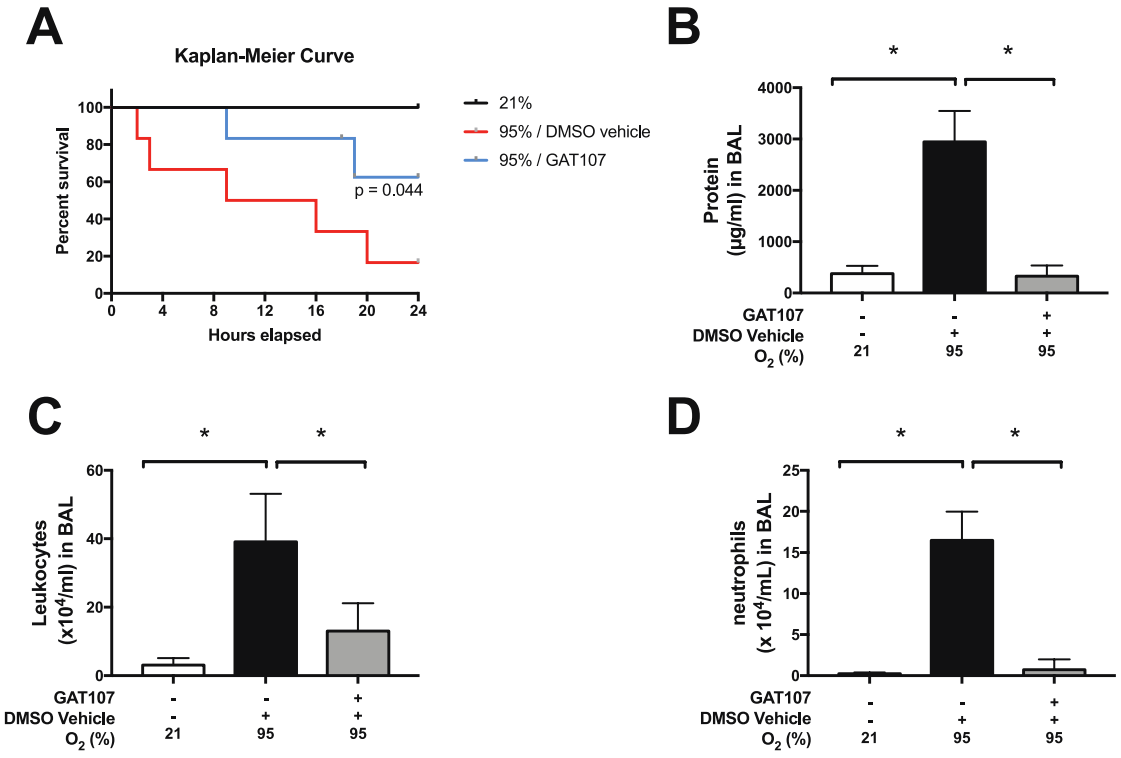


**Fig. 1. Systemic administration of GAT107 increases probability of survival and attenuates inflammatory lung injury in mice exposed to hyperoxia and PA lung infection.** Male C57BL/6 were exposed to either 21% O2 (room air) or >95% O2 (hyperoxia) for 72 h, inoculated with PA (0.1 × 108 CFUs/mouse), and then returned to an environment of 21% O2 after inoculation. Hyperoxic mice were randomized to receive either GAT107 (3.3 mg/kg) or vehicle control intraperitoneally, every 12 h, starting at hour 24 of hyperoxia. **(A)** After mice were inoculated, animal survival was monitored and recorded every hour for 24 h and the percentage of mice that survived is shown in the Kaplan-Meier curve. Data was analyzed using the log-rank Mantel-Cox test (n = 5–10 mice/group). **(B)** BAL samples were harvested 24 h after PA inoculation. The total protein content in the BAL samples was quantified using bicinchoninic acid (BCA) assay. **(C)** The number of leukocytes was determined in BAL samples using a hemocytometer. **(D)** A differential cell counting analysis was used to determine the number of neutrophils following the staining of neutrophils with cytospin and Hema3 staining. Data represents the mean ± SEM from two-independent experiments (n = 6 mice per group). *p < 0.05 compared to hyperoxia exposed vehicle treated control group.

collected. Fig. 1 shows that mice exposed to hyperoxia and challenged with PA (vehicle control group) had significantly higher levels of protein in their airways (2944.52 ± 247.07 μg protein/mL, $p < 0.05$), total airway leukocyte infiltrates (39.1 ± 6.28 × $10^4$ cells/mL, $p < 0.05$), and infiltrated neutrophils (16 ± 2.01 × $10^4$ cells/mL, $p < 0.05$), compared to mice that remained at 21% $O_2$ (379.84 ± 55.97 μg protein/mL, 3.12 ± 1.01 × $10^4$ leukocytes/mL, and 0.247 ± 0.09 × $10^4$ neutrophils/mL), and these results were consistent with the study of Patel et al. (2013) [15]. However, mice given 3.3 mg/kg i.p. of GAT107 had significantly lower levels of airway protein content and total leukocyte and neutrophil infiltrates (329.59 ± 91.21 μg protein/mL, 13.00 ± 4.08 × $10^4$ leukocytes/mL, and 0.73 ± 0.73 × $10^4$ neutrophils/mL, respectively, $p < 0.05$), compared to mice given the vehicle. These data suggest that GAT107 can protect mice in our mouse model of VAP from acute inflammatory lung injury and increase their survival.

### 3.3. GAT107 significantly decreases airway accumulation of HMGB1 in hyperoxia-exposed mice with P. aeruginosa (PA) lung infection

Excessive levels of HMGB1 in the airways and lungs of mice play a critical role in the pathogenesis of hyperoxia-induced inflammatory lung injury [37]. Therefore, we conducted experiments to determine if the systemic administration of GAT107 attenuates the accumulation of HMGB1 in the airways of mice exposed to hyperoxia and PA. Mice were exposed to 95% $O_2$ for 48 h. During the 48 h of hyperoxia exposure, mice were given 3.3 mg/kg i.p. of GAT107 or vehicle (DMSO). After 48 h, mice were challenged with intratracheal PA. After 24 h, BAL fluids were collected and the level of HMGB1 was determined using western blot assays. As shown in Fig. 2A, mice that were exposed to 95% $O_2$ hyperoxic conditions and intratracheally challenged with PA had significantly higher levels of HMGB1 in the airways (6350.5 ± 805.1 A U. HMGB1, $p < 0.01$), compared to mice that remained in 21% $O_2$ room air (3637.4 ± 469.5 A U. HMGB1). The administration of 3.3 mg/kg i.p. of GAT107 significantly decreased the accumulation of airway HMGB1 in mice exposed to hyperoxia and PA lung infection (762.7 ± 190.1 A U. HMGB1, $p < 0.001$), compared to vehicle-treated mice. These data suggest that GAT107 protects mice in this VAP model from acute inflammatory lung injury, in part, by decreasing the airway accumulation of HMGB1.

### 3.4. GAT107 significantly decreases the accumulation of extracellular HMGB1 in cell culture media and protects against HMGB1-induced phagocytic dysfunction

The prolonged exposure of patients and mice to hyperoxia causes the accumulation of HMGB1 in the airways, which is a potent pro-inflammatory mediator that impairs macrophage functions [15,37,63]. To determine if GAT107 decreases hyperoxia-induced HMGB1 release from macrophages under hyperoxic conditions, RAW 264.7 cells were exposed to >95% $O_2$ for 24 h, in the presence of either 3.3 μM of GAT107 or vehicle (DMSO). Western blot analysis of the culture media from macrophages exposed to hyperoxia indicated a significant increase in extracellular HMGB1 (119.18 ± 18.89%, $p < 0.05$), compared to macrophages that remained at room air (21% $O_2$) (8.003 ± 4.68%). The hyperoxia-induced increase in extracellular HMGB1 levels was significantly decreased following incubation with 3.3 μM of GAT107 (39.8 ± 8.54%, $p < 0.05$) (Fig. 2B), when normalized to macrophages exposed to hyperoxia and incubated with vehicle in the absence of GAT107 (119.18 ± 18.89%).

It has been reported that the excessive accumulation of extracellular HMGB1 in the airways mediates the impairment of macrophage functions [15,21,37,38]. To determine if GAT107 attenuates HMGB1-induced macrophage phagocytic dysfunction, RAW 264.7 cells were incubated with 10 μg/mL of recombinant HMGB1 (rHMGB1) for 24 h, in the presence or absence of GAT107 (3.3 μM) or the vehicle (DMSO). Similar to hyperoxia-compromised macrophages, macrophages incubated with rHMGB1 had impaired phagocytic function, compared to macrophages incubated with vehicle (47.65 ± 1.62% vs. 100%, $p < 0.05$). However, HMGB1-compromised macrophage phagocytic function was significantly attenuated following incubation with 3.3 μM of GAT107 (66.32 ± 0.21%, $p < 0.05$) (Fig. 2D), compared to macrophages incubated with rHMGB1 and the vehicle. These results indicate that GAT107 significantly 1) decreases the accumulation of HMGB1 airway levels released from macrophages exposed to hyperoxia

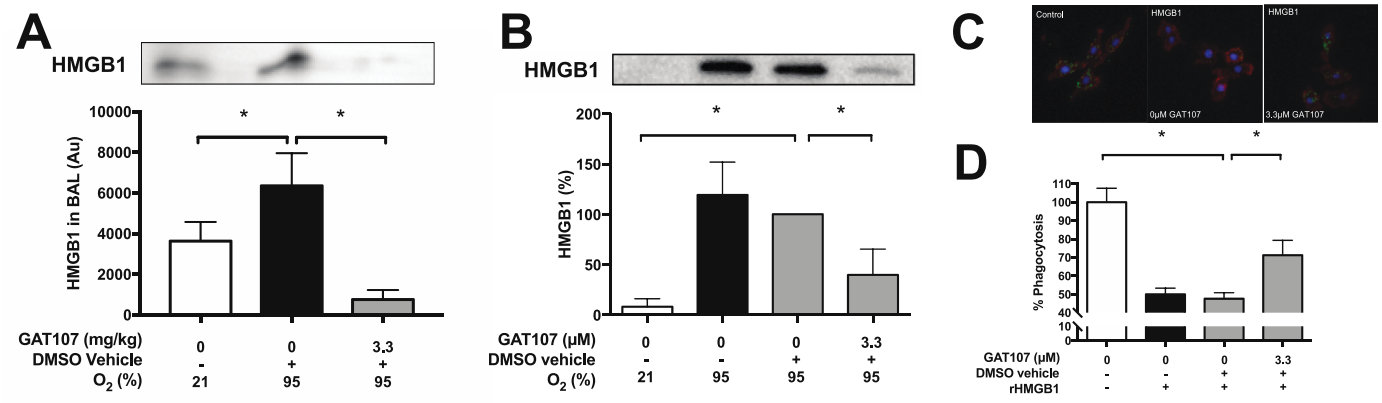


**Fig. 2. GAT107 significantly attenuates hyperoxia-induced accumulation of extracellular HMGB1 and HMGB1-induced macrophage dysfunction. (A)** Male C57BL/6 mice were exposed to either 21% O2 (room air) or >95% O2 (hyperoxia) for 48 h and then inoculated with PA (0.1 × 108 CFUs/mouse) and were returned to 21% O2 after inoculation. Hyperoxic mice were randomized to receive GAT107 (3.3 mg/kg) or vehicle control (1 mL/kg), intraperitoneally, every 12 h starting at hour 24 of hyperoxia. BAL was harvested 24 h after inoculation and western blot assays were conducted to determine the levels of extracellular HMGB1 in BAL. A representative western blot of HMGB1 is presented and HMGB1 levels were quantified using western blot analysis. **(B)** RAW 264.7 macrophages were either cultured in room air (white bar) or exposed to hyperoxia (black bar) without or with GAT107 in DMSO (grey bars). After 24 h, cell culture supernatant was collected and the level of extracellular HMGB1 was determined using western blot analysis. A representative western blot of HMGB1 is presented (B) and HMGB1 levels were quantified using western blot analysis. **(*C*–D)** RAW 264.7 macrophages were either exposed to vehicle control (white bar) or 10 μg/mL of HMGB1 (black bar) without or with 3.3 μM GAT107 (grey bars). Cells were incubated with fluorescein isothiocyanate (FITC)-labeled mini-beads for 1 h and stained with rhodamine phalloidin and DAPI to visualize the cytoskeleton and nucleus. Immunofluorescent micrographs show the phagocytosed beads (green), cytoskeleton (red), and DNA in the nucleus (blue) of RAW 264.7 cells following their incubation with HMGB1. Fluorescent micrographs were quantified using ImageJ for phagocytic activity and represented as percent of beads phagocytosed per macrophage in a bar graph (n = 3). The bar graphs represent the quantification of phagocytosis of at least 200 cells. Each value represents the mean ± SEM of three independent experiments for each group. *p < 0.05, versus the 95% O2 vehicle control group.

and 2) inhibits macrophage dysfunction caused by airway HMGB1.

### 3.5. GAT107 significantly decreases hyperoxia-induced NF-κB activation and extracellular levels of TNFα

Previously, we have reported that hyperoxia-induced NF-κB activation plays a critical role in the release of HMGB1 from hyperoxic macrophages [39]. Consequently, in these experiments, we determined the effect of GAT107 on the activation of NF-κB, a known mediator of inflammation that causes the release of HMGB1 from cells, such as macrophages [17,39,40]. The exposure of macrophages to hyperoxia significantly increased NF-κB activation (1.5 ± 0.006-fold, $p < 0.05$), compared to macrophages exposed to room air (1.00 ± 0-fold). The incubation of hyperoxia-exposed macrophages with 3.3 μM of GAT107 significantly decreased (1.19 ± 0.005-fold, $p < 0.05$) the hyperoxia-induced increase in NF-κB (p65 subunit) binding to DNA, compared to the vehicle (1.47 ± 0.005-fold) (Fig. 3A). Furthermore, the transcription activation of NF-κB by HMGB1 increases the production and secretion of TNFα [41]. As shown in Fig. 3B, macrophages exposed to hyperoxia had a significantly greater accumulation of TNFα in their culture media, compared to macrophages exposed to room air (107.15 ± 14.94%, $p < 0.05$ versus 54.84 ± 3.24%). In addition, GAT107 significantly decreased the levels of extracellular TNFα at 3.3 μM (60.26 ± 14.08%, $p < 0.05$), compared to vehicle control (107.15 ± 14.94%).

### 3.6. GAT107 significantly decreases hyperoxia-induced mitochondrial membrane hyperpolarization and the accumulation of mitochondrial superoxide

The exposure of macrophages to hyperoxia produces mitochondrial damage [31,42]. Furthermore, mitochondrial damage significantly inhibits macrophage phagocytosis [43]. To determine if 24 h exposure of macrophages to hyperoxia affects mitochondrial function, the mitochondrial membrane potential was determined using the tetramethylrhodamine ethyl ester (TMRE) assay. The results indicated that the mitochondrial membrane potential of macrophages exposed to hyperoxia was hyperpolarized (141 ± 13.8%, $p < 0.05$), compared to macrophages exposed to room air control (100%) (Fig. 4A). However, hyperoxia-induced mitochondrial hyperpolarization was significantly decreased by 3.3 μM of GAT107 (62.85 ± 7.29%, $p < 0.05$), compared to the vehicle (123.5 ± 4.6%) (Fig. 4A). Furthermore, the prolonged exposure to hyperoxia also significantly increased the mitochondrial levels of superoxide (mitoSOX) (212 ± 23%, $p < 0.05$), when normalized to that from macrophages that remained in room air (21% $O_2$) (100%) (Fig. 4B). GAT107, at 3.3 μM, significantly decreased (147.7 ± 33.4%, $p < 0.05$) the hyperoxia-induced increase in mitoSOX levels, compared to hyperoxia-compromised macrophages incubated with vehicle (226.3 ± 31%) (Fig. 4B). Therefore, these results suggest that GAT107 decreases hyperoxia-induced mitochondrial membrane damage by decreasing hyperoxia-induced accumulation of superoxide in mitochondria.

### 3.7. GAT107 significantly attenuates hyperoxia-compromised MnSOD activity

Under normal cellular conditions, mitoSOX is rapidly dismutated into hydrogen peroxide by MnSOD [44]. To determine if hyperoxia exposure affects the total levels of MnSOD protein expression in macrophages, western blot analysis was performed on macrophage lysate collected from RAW 264.7 cells exposed to 24 h of hyperoxia and incubated with GAT107. Interestingly, in macrophages exposed to hyperoxic conditions, there was a significant increase in the total level of MnSOD protein (2.93 ± 0.18 MnSOD/actin, $p < 0.05$), compared to macrophages that remained in room air (1.17 ± 0.23 MnSOD/actin) (Fig. 5B). Furthermore, incubation with 3.3 μM of GAT107 did not significantly (2.89 ± 0.13 MnSOD/actin) alter the hyperoxia-increase in MnSOD protein, compared to the vehicle (2.78 ± 0.15 MnSOD/actin). Therefore, we postulated that the significant increase in mitoSOX following prolonged exposure to hyperoxia could not result from an alteration in the protein levels of MnSOD (Fig. 5).

To determine if GAT107 modulated MnSOD activity under hyperoxic conditions, macrophage whole cell lysate was collected and subjected to MnSOD enzyme activity assay. As shown in Fig. 5C, macrophages exposed to hyperoxic conditions had significantly lower MnSOD activity (2.72 ± 0.11 U/mg protein, $p < 0.05$), compared to macrophages that remained in room air (3.9 ± 0.2 U/mg protein). Interestingly, the incubation of hyperoxia-exposed macrophages with 3.3 μM of GAT107 significantly increased MnSOD activity, (3.26 ± 0.047 U/mg, $p < 0.05$), compared to macrophages incubated with the vehicle (2.73 ± 0.09 U/mg) (Fig. 5C). These data indicated that GAT107 attenuates hyperoxia-induced MitoSOX by increasing MnSOD activity, independent of its protein levels.

### 3.8. GAT107 restores MnSOD activity by inhibiting hyperoxia-induced glutathionylation of MnSOD

Previous studies have reported that in oxidative stress environments, MnSOD undergoes post-translational modification that decreases its catalytic activity [44]. MnSOD activity was not dependent on the levels of the MnSOD protein as GAT107 did not significantly alter MnSOD activity, compared to the hyperoxia control group (Fig. 5). Therefore, we determined the effect of GAT107 on the post-translational glutathionylation of MnSOD, which could affect MnSOD activity. Western blot analysis of co-immunoprecipitated MnSOD indicated that macrophages exposed to hyperoxia had significantly higher levels of glutathionylated MnSOD, compared to macrophages exposed to room air (91.8 ± 6.7% versus 7.6 ± 4.5% GSH/MnSOD, $p < 0.05$) (Fig. 6B). Macrophages exposed to hyperoxia in the presence of 3.3 μM of GAT107 had a significantly lower level of glutathionylated MnSOD, compared to macrophages incubated with vehicle (53.5 ± 7.5% versus 91.2 ± 6.5%

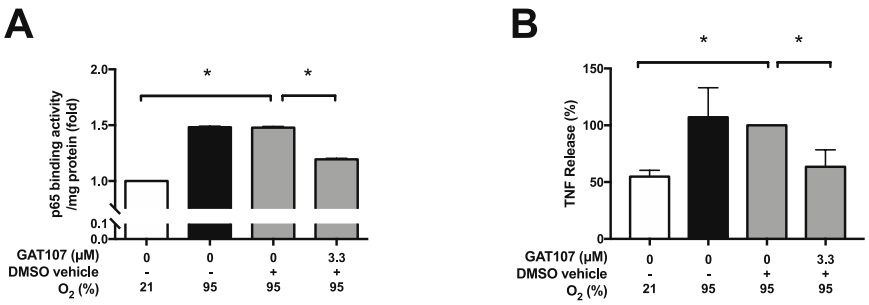


**Fig. 3. GAT107 significantly attenuates hyperoxia-induced NF-kB activation and increases extracellular TNFa levels.** RAW 264.7 macrophages were either exposed to 21% O2 (room air, white bar) or >95% O2 (hyperoxia, black bar) without or with GAT107 (grey bars). After 24 h, **(A)** cell lysates were collected and analyzed for NF-kB (p65 subunit) binding activity to DNA by ELISA using a NF-**k**B Transcription Factor Activity Kit and the results are represented as a bar graph; **(B)** cell culture supernatant was collected and analyzed for the levels of TNF**a** using ELISA. The bar graph represents the relative amounts of TNF**a** present in the cell culture media, compared to vehicle control. Each value represents the mean ± SEM of three independent experiments for each group. *$p < 0.05$, versus 0 μM (vehicle control).

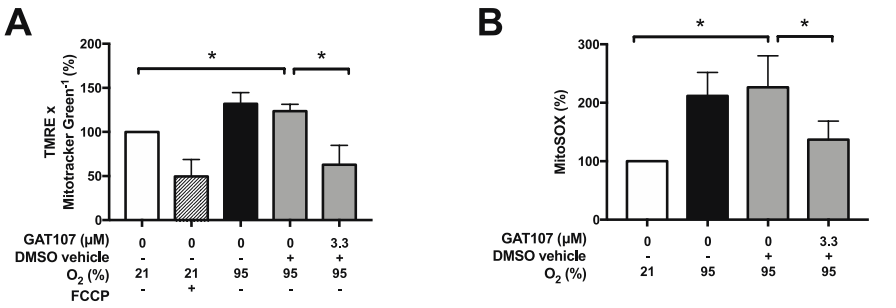


**Fig. 4. GAT107 decreases hyperoxia-induced mitochondrial membrane hyperpolarization and the accumulation of mitochondrial superoxide.** RAW 264.7 macrophages were either exposed to 21% O2 (room air, white bar) or 95% O2 (hyperoxia, black bar) without or with GAT107 (grey bars). After 24 h, **(A)** macrophage mitochondrial integrity was determined using the tetramethylrhodamine, ethyl ester (TMRE) mitochondrial membrane potential assay that was normalized to MitoTracker Green. **(B)** The levels of mitochondrial superoxide in macrophages were analyzed using the MitoSOX dye assay at 24 h of hyperoxia. Each value represents mean ± SEM of three independent experiments for each group. *p < 0.05, versus the hyperoxia exposed vehicle treated control group.

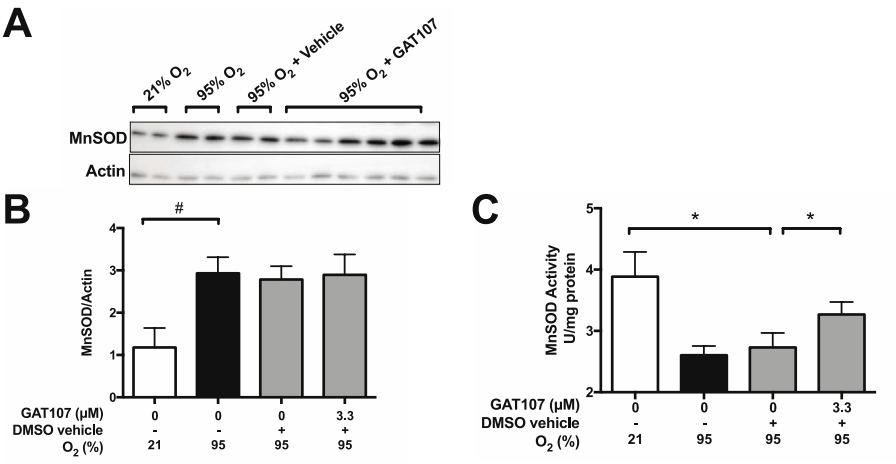


**Fig. 5. GAT107 attenuates hyperoxia-compromised MnSOD activity.** RAW 264.7 macrophages were either exposed to 21% O2 (room air, white bar) or 95% O2 (hyperoxia, black bar) without or with GAT107 (grey bars). After 24 h, whole cell lysates were analyzed for total MnSOD levels using western blot assays for MnSOD. **(A)** Representative western blots for MnSOD and actin are presented, and **(B)** MnSOD and actin levels were quantified using western blot analysis. **(C)** RAW 264.7 macrophage cell lysate was used to determine MnSOD activity, using a SOD activity kit in the presence of cyanide. Each value represents mean ± SEM of three independent experiments for each group. #p < 0.05, versus the room air control group; *p < 0.05, versus the hyperoxia exposed vehicle treated control group.

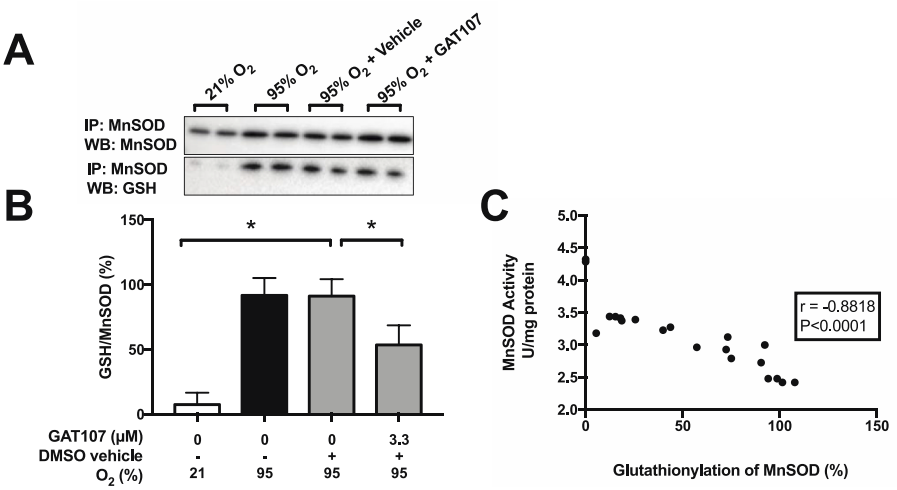


**Fig. 6. The hyperoxia-induced glutathionylation of MnSOD was significantly decreased by GAT107.** RAW 264.7 macrophages were either exposed to 21% O2 (room air, white bar) or 95% O2 (hyperoxia, black bar) without or with GAT107 (grey bars). After 24 h, whole cell lysates were co-immunoprecipitated for MnSOD. **(A)** Representative western blots for immunoprecipitated MnSOD and conjugated GSH. **(B)** Densiometric analysis for immunoreactive GSH and MnSOD bands were determined and the ratio of glutathione (GSH) to MnSOD was reported as a percentage on the bar graph. Each value represents the mean ± SEM of 3–4 independent experiments for each group. *p < 0.05, versus hyperoxia exposed vehicle control group. **(C)** MnSOD activity of the samples compared to their corresponding percentage of MnSOD glutathionylation presented as a correlation plot. Each value on the correlation plot represents individual sample data points from 3 to 4 independent experiments. The measure of strength between the X and Y variables was determined by a two-tailed Pearson-correlation coefficient, which computed a p < 0.0001 between MnSOD activtabity and percentage of MnSOD glutathionylation.

GSH/MnSOD, $p < 0.05$) (Fig. 6B). Correlation analysis indicated a significant negative correlation between an increase in the glutathionylation of MnSOD and MnSOD activity (correlation coefficient, $r = -0.8818$, $p < 0.0001$) (Fig. 6C). Thus, in the presence of 3.3 μM of GAT107, glutathionylation of MnSOD was significantly decreased, resulting in a corresponding increase in MnSOD activity. These results indicate that the activation of α7nAChRs significantly increases the antioxidant capacity of mitochondria.

## 4. Discussion

In this study, our results indicated that GAT107 significantly

increases the survival rates of mice exposed to hyperoxia and inoculation with PA via intratracheal instillation. The rescue effects produced by GAT107 were negatively correlated with a significant decrease in hyperoxia-induced inflammatory lung markers, such as a decrease in lung permeability (decrease in total lung protein content) and the decrease in total leukocyte and neutrophil lung infiltration (Fig. 1). This improved outcome in this mouse model of VAP was due, in part, to 1) decreasing the accumulation of airway HMGB1 and its downstream signaling pathway and 2) increasing mitochondria integrity by decreasing hyperoxia-induced mitochondria oxidative stress, via inhibiting the glutathionylation of MnSOD.

### *4.1. GAT107 increases survival and decreases acute inflammatory lung injury*

Since 1899, numerous studies in humans have shown that exposure to hyperoxia promotes the pathogenesis of pneumonia and lung injury [4,6,45,46]. Unfortunately, approximately one-third of mechanically ventilated ICU patients develop VAP, which has a 4.6% mortality rate [34,35,47]. Importantly, there is a positive correlation between the length of mechanical ventilation and the incidence of patient mortality in ICU [48]. Hyperoxia-induced toxicity increases inflammatory responses and aging biomarkers, primarily due to the increased levels of ROS and cellular redox imbalance [4,45]. Furthermore, prolonged exposure to hyperoxia causes hyperoxia-induced acute lung injury, characterized by increased airway protein content and inflammatory cell infiltration, which is mediated, in part, by oxidative stress and the extracellular accumulation of HMGB1 [5,15,17,37]. Previously, it has been reported that the activation of the cholinergic anti-inflammatory pathway protects against shock-induced death and lung injury in dogs by decreasing vaso-permeability and the secretion of TNFα and IL-1α [49]. The activation of the α7nAChR-mediated cholinergic anti-inflammatory pathway decreases hyperoxia-induced lung inflammation via the vagus nerve, which eventually restores compromised neuroimmunomodulation and increases lung immune homeostasis and neurocognitive functions [17,28,45,50,51]. The partial α7nAChR agonist, GTS-21, has been reported to have a protective effect against hyperoxia and LPS-induced lung injury by decreasing the pro-inflammatory response of macrophages [17,20,51]. Therefore, it is possible that patients who receive prolonged oxygen therapy, such as those on mechanical ventilation, may benefit from the treatment with activators of the cholinergic anti-inflammatory pathway, such as GTS-21 and GAT107, as inflammatory lung injury would be decreased and this could increase survival of these patients. Importantly, as mentioned earlier, the duration of mechanical ventilation is correlated with the incidence of mortality in ICU patients [48]. Thus, it is possible that GAT107 may improve the probability of survival by decreasing pulmonary inflammation, lung permeability/edema and lung injury. It is possible that treatments such as GAT107 could allow clinicians to use conservative oxygen strategies and/or reduce the number of days that a patient needs to be mechanically ventilated [52].

### *4.2. GAT107 protects mouse lungs and macrophages from the accumulation of extracellular HMGB1 and protects against HMGB1-induced phagocytic dysfunction*

The i.p. administration of 3.3 mg/kg of GAT107 significantly decreased the accumulation of HMGB1 in the airways of hyperoxia-exposed mice inoculated intratracheally with PA (Fig. 2). This finding was consistent with our previous study using GTS-21, which significantly decreased HMGB1 accumulation in the airways of mice exposed to hyperoxia either alone or in the presence of PA lung infection [17,51]. HMGB1, a non-histone chromosomal protein, is present in the nucleus under normal conditions [53–56]. Immune cells may release HMGB1 when damaged or stressed and this induces its cytoplasmic translocation, and ultimately, release into the extracellular milieu [63]. HMGB1 can bind to pattern recognition receptors (PRRs) to induce a pro-inflammatory cascade, followed by the downstream activation and nuclear translocation of NF-κB [55,57–59]. In hyperoxia-exposed mice, GTS-21 prevented the nuclear-to-cytoplasmic localization of HMGB1 in alveolar epithelial cells and macrophages [17,51], a critical step in the active secretion of HMGB1 [63]. In addition, GTS-21 also decreased the systemic increase of extracellular HMGB1 produced by hyperoxia [17]. Thus, GAT107, after i.p. administration, may be acting on multiple cell types to decrease the levels of HMGB1 in the airways of animals exposed to hyperoxia. Nonetheless, alveolar macrophages are the main resident inflammatory cells in the lung that are one of the major sources of extracellular HMGB1 in the lungs [63]. Interestingly, alveolar macrophages in patients with severe acute respiratory coronavirus-2 (SARS-CoV-2) pneumonia have been reported to be central mediators of the lung hyper-inflammatory response [60].

In this study, 3.3 μM of GAT107 significantly reduced (65–70%) the hyperoxia-induced extracellular accumulation of HMGB1 in the media of cultured macrophages (Fig. 2). Previously, GTS-21, at 25 and 50 μM, also decreased hyperoxia-induced HMGB1 extracellular accumulation by 50–60%, and this was mediated, in part, by a decrease in NF-κB activation [51]. Our results indicated that GAT107 did not completely decrease the release and extracellular accumulation of HMGB1 from hyperoxia-compromised macrophages. Although GAT107 significantly decreased the extracellular levels of HMGB1, it is possible that the remaining extracellular HMGB1 produces phagocytic dysfunction [21]. As shown in Fig. 2, 3.3 μM of GAT107 significantly protected macrophages against HMGB1-induced phagocytic dysfunction and almost completely reversed the hyperoxia-induced decrease in the phagocytotic activity of cultured macrophages [28]. However, the biology of HMGB1 is rather complicated and the functions of HMGB1 are dependent on its location, concentration, and translational modifications. While nuclear HMGB1 is involved in the regulation of DNA transcription and DNA repair, extracellular HMGB1 can function as a potent inflammatory cytokine, facilitating the infiltration of immune cells, including neutrophils, monocytes, and T cells, to the sites of infections, thus inducing cellular damage and/or tumorigenesis [61,62,63]. Thus, depleting extracellular HMGB1 could be problematic under such conditions. However, excessive levels of extracellular HMGB1 can induce an exaggerated secretion of numerous proinflammatory cytokines, thereby compromising macrophage functions [21,61,63], resulting in infection-induced pneumonia, severe inflammatory acute lung injury, and even acute respiratory distress syndrome (ARDS) in severe cases of COVID-19 patients. Therefore, it is rational to modulate, instead of depleting, the levels of extracellular HMGB1.

Numerous clinical studies indicate that inflammation and oxidative stress are the primary clinical manifestations of COVID-19 [55]. It is likely that GAT107 alters HMGB1-induced downstream signaling that is involved in the propagation of inflammation, intracellular oxidative stress and phagocytic dysfunction [63]. In a clinical observational study conducted by Passos et al. (2022) [55], oxidative stress markers, such as glial fibrillary acidic protein (GFAP), receptor for advanced glycation end products (RAGE), HMGB1 and cyclo-oxygenase-2 (COX-2), were measured to evaluate their role in COVID-19 pathogenesis, in 93 patients from Sergipe, Brazil. The results indicated a significant increase in the GFAP and GFAP breakdown product, GFAP-BP, in COVID-19 patients admitted to ICU and critical COVID-19 patients, compared to outpatients (GFAP: 1:22 [0.97–1.66], 1.07 [0.60–1.30], GFAP-BP: 1.16 [0.97–1.43], 0.74 [0.59–1.21] respectively). Furthermore, the level of GFAP-BP was significantly increased in ICU patients/critically ill patients, compared to healthy controls (GFAP: 1.22 [0.97–1.66], 0.86 [0.61–1.13], GFAP-BDP: 1.16 [0.97–1.43], 0.67 [0.51–0.82] respectively).

Extracellular HMGB1 binds with high affinity to negatively charged pathogens and damage-associated molecular patterns (DAMPs), such as LPS, DNA, and viral RNA [64]. The binding of HMGB1 to LPS allows for the RAGE-mediated endocytosis of HMGB1-LPS complexes and the

activation of intracellular receptors that initiate inflammatory cytokine production, inflammasome, and pyroptosis activation [64]. Importantly, when cultured macrophages are incubated with α7nAChR agonists or acetylcholine, macrophage immune activation is prevented by inhibiting the endocytosis of HMGB1 and HMGB1 complexed with LPS [65]. However, the exact mechanism by which GTS-21 or acetylcholine inhibits the endocytosis of HMGB1 and HMGB1-LPS complexes remains to be elucidated. There are current ongoing COVID-19 clinical trials that are evaluating activators of the cholinergic anti-inflammatory pathway (such as nicotine, an α7nAChR agonist), as it is possible they can attenuate the COVID-19 cytokine release syndrome by decreasing the cellular endocytosis of HMGB1-SARS-CoV-2 RNA complexes [66].

Extracellular HMGB1 can also activate toll-like receptor 4 (TLR4) on macrophages, eliciting downstream signaling involved in pro-inflammatory cytokine production, which further increases HMGB1 release, thus creating a deleterious feedback cycle [19,21,63]. Passos et al. (2022) reported a significant increase in RAGE immunocontents in COVID-19 patients admitted to the ICU, compared to those previously infected with SARS-CoV-2 and healthy controls (1.11 [0.96–1.43], 0.71 [0.53–1.03], 0.61 [0.46–1.05]) [55]. GAT107, by activating α7nAChR, could attenuate these HMGB1-PRR-mediated deleterious effects by increasing the levels of the protein, interleukin-1 receptor-associated kinase-M (IRAK-M). Maldifassi et al. (2014) previously reported that after α7nAChR activation, IRAK-M upregulation occurs, a negative regulator of TLR4-mediated downstream pro-inflammatory cytokine upregulation [23,67]. Furthermore, in the same study, the knockdown of the IRAK-M gene significantly decreased the efficacy of nicotine in decreasing the LPS-induced secretion of TNFα from human macrophages.

### 4.3. GAT107 decreases hyperoxia-induced NF-κB activation and TNFα secretion

GAT107 also significantly decreased the hyperoxia-induced activation of NF-κB and the release of TNFα into culture media (Fig. 3). The active release of HMGB1 from macrophages has been previously reported to be due, in part, to the activation of NF-κB by hyperoxia [17,39]. In addition, NF-κB is also a critical transcription factor for TNFα [68]. As an early mediator of inflammation, TNFα is also present in the airways of critically ill VAP patients, at concentrations up to 1303 ng/mL [69,70]. Importantly, TNFα, in combination with HMGB1, plays a critical role in mediating lung inflammation and injury [63,68]. Once in the extracellular milieu, HMGB1 can activate autocrine-like pathways that further increase the production and secretion of TNFα and HMGB1 [63]. Thus, targeting NF-κB activation can interrupt or blunt this HMGB1 deleterious feedback cycle that causes excessive inflammation. Indeed, GTS-21 increases bacterial clearance and survival in a mouse model of VAP by decreasing the NF-κB-induced release of HMGB1 and its accumulation in the airways [17]. Under normoxic conditions, HMGB1 remains in the nucleus and is a non-chromosomal DNA binding protein [19,63]. Upon stimulation by LPS or oxidative stress, HMGB1 is released from macrophages by translocating from the nucleus to the cytoplasm, where it is released by endolysosomes into the extracellular milieu [71–73]. NF-κB activation induces the translocation of HMGB1 from the nucleus to the cytoplasm [17]. The release of HMGB1 from cells may also involve the activation of pathways distinct from NF-κB. Lu et al. (2014) reported that inflammasome activation induces the active release of HMGB1 from macrophages [74]. Furthermore, in the same study, GTS-21 significantly decreased inflammasome-mediated release of HMGB1 [74]. GAT107 significantly decreased hyperoxia-induced HMGB1 release and extracellular accumulation of cultured macrophages. GAT107 had greater efficacy in decreasing inflammasome- and hyperoxia-induced HMGB1 release at concentrations significantly lower than GTS-21, which may be due to GAT107's potent ago-PAM activation of α7nAChR, compared to partial agonists, such as GTS-21.

### 4.4. Hyperoxia disrupts mitochondrial membrane integrity

As shown in Fig. 4, mitochondrial membrane hyperpolarization occurs in macrophages exposed to 24 h of hyperoxia. Furthermore, mitochondrial hyperpolarization may indicate a dysregulation of oxidative phosphorylation, which increases ROS generation and the subsequent loss of ATP production [75,76]. There are at least ten known sites in mitochondria that produce ROS [71,77–79]. However, it has been reported that in the presence of high levels of oxygen, the mitochondrial flavoprotein, quinone oxidoreductase, may be the only source of ROS [80]. In mice exposed to 72 h of hyperoxia, there was a significant inhibition of complex I activity (which produces ROS) and decreased ATP production in isolated pulmonary mitochondria [81]. In this study, GAT107 significantly decreased hyperoxia-induced macrophage mitochondrial hyperpolarization. Therefore, by normalizing the mitochondrial membrane potential, GAT107 is involved in the maintenance of mitochondrial integrity and this establishes conditions reported in normal mitochondria.

### 4.5. GAT107 decreases the hyperoxia-induced decrease in MnSOD activity

Under normal physiological conditions, MnSOD catalyzes the dismutation reaction of mitochondrial superoxide into hydrogen peroxide, at a rate of $2 \times 10^9$ $M^{-1}s^{-1}$, and hydrogen peroxide is rapidly biotransformed to water by catalase [44,82,83]. However, as shown in Fig. 5, 24 h of hyperoxia exposure significantly decreased MnSOD activity. Other studies have reported that the intermittent exposure of macrophages to hyperoxia for 7 days significantly decreased MnSOD function at 7 days, but interestingly, after 3 weeks, MnSOD function was significantly increased [84]. In contrast, in guinea pigs exposed to hyperoxia for 3 days, alveolar macrophage MnSOD function was significantly increased [85]. However, in cultured macrophages overexpressing MnSOD or after incubation with exogenous SOD, macrophages had significantly greater phagocytic capacity for PA after exposure to 24 h of hyperoxia [86,87].

In our study, GAT107 restored mitochondrial function, as indicated by the normalization of mitochondrial membrane potential (Fig. 4). GAT107 also normalized mitochondrial superoxide levels (Fig. 4). The GAT107-mediated normalization of mitochondrial superoxide levels was significantly correlated with attenuated hyperoxia-compromised MnSOD activity (Fig. 5), suggesting that excessive levels of mitochondrial superoxide may result from MnSOD dysfunction. Moreover, GAT107's restoration of MnSOD activity was not dependent on the overall protein levels of MnSOD (Fig. 5). Interestingly, in cultured macrophages exposed to 3-weeks of intermittent hyperoxia, macrophages survived only if they expressed significantly higher levels of MnSOD activity [84]. Therefore, since GAT107 did not significantly alter the total protein levels of MnSOD, it suggests that MnSOD activity is not being modulated at the protein level. Therefore, it is possible that GAT107 may be increasing MnSOD activity by affecting post-translational modifications [88]. Indeed, studies have reported that post-translational modifications of MnSOD significantly alter its enzymatic function [44,89–93]. The glutathionylation of proteins has been reported to have a protective role against irreversible oxidative modifications (e.g., sulfonic acid) of reactive cysteine residues [94]. Our results indicated that hyperoxia induces the glutathionylation of MnSOD and this was significantly decreased by incubating macrophages with 3.3 μM of GAT107. Furthermore, the increase in MnSOD glutathionylation was significantly correlated with decreased MnSOD activity (Fig. 6), indicating that glutathionylation of MnSOD modulates its enzymatic activity. Previously, it has been reported that under oxidative stress conditions, non-mitochondrial CuZnSOD is glutathionylated at Cys111 and FeSOD is glutathionylated at Cys57 [44]. Currently, it remains to be determined how GAT107 decreases the glutathionylation of MnSOD. We postulate that GAT107 may be decreasing MnSOD

glutathionylation through pathways that augment the mitochondrial antioxidant capacity, thereby decreasing the oxidative burden on MnSOD by the GAT107-induced activation of the Nrf2/HO-1 pathway [28]. Also, the upregulation of heme oxygenase-1 (HO-1) can cause its translocation to mitochondria from the cytoplasm. In human lung epithelial cells exposed to particulate matter that is 2.5 μm (PM2.5) in diameter, there was a significant increase in the preferential transposition of HO-1 into the mitochondria, which may play a protective role in PM2.5-induced necrosis [95]. The activation of α7nAChR by acetylcholine or GTS-21 results in the downstream Nrf2 activation and the transcriptional upregulation of antioxidants such as glutathione [22,23,96–98]. It is likely that under oxidative stress conditions, non-enzymatically and enzymatically catalyzed glutathionylation reactions occur in the mitochondria, since the mitochondrial concentration of glutathione is approximately 5–10 mM [99]. In addition, the de-glutathionylation of proteins may be facilitated by sulfiredoxins, glutaredoxin 2 (Grx2) and thioredoxin (Trx) [94,100,101]. Thus, GAT107 could affect the de-glutathionylation of proteins by acting on one of these de-glutathionylating enzymes, although this remains to be determined. It is likely that hyperoxia-induced lung injury results from dysregulation of proteins that maintain the glutathionylation status of proteins, as dysregulation of glutathionylation has been linked to lung diseases, such as idiopathic pulmonary fibrosis, asthma, and chronic obstructive pulmonary disorder [101]. Therefore, the activation of α7nAChR by GAT107 could be a potential therapeutic option for patients with various lung diseases and disorders.

## 5. Conclusion

In this article, we report that the novel α7nAChR agonistic positive allosteric modulator (ago-PAM), GAT107, significantly increased the probability of survival by decreasing acute inflammatory lung injury in a mouse model of VAP. Mechanistically, GAT107 decreased the accumulation of extracellular HMGB1 in the airways by inhibiting its release from hyperoxic lung cells, including macrophages, and by attenuating HMGB1-mediated macrophage dysfunction. Furthermore, hyperoxia can impair mitochondrial integrity by increasing the levels of ROS and decreasing MnSOD activity, which is caused by glutathionylation. GAT107 decreased hyperoxia-induced mitochondrial damage and increased MnSOD activity by decreasing hyperoxia-induced MnSOD glutathionylation. GAT107 restored macrophage functions by modulating the glutathionylation status of MnSOD. Therefore, GAT107, by activating α7nAChR, may be a potential treatment for oxidative stress-induced inflammatory lung injury by improving the clinical outcome in patients on oxygen therapy.

## Declaration of competing interest

The authors declare that they have no known competing financial interests or personal relationships that could have appeared to influence the work reported in this paper.

## Data availability

Data will be made available on request.

## Acknowledgments

The authors would like to thank Dr. Ravi Sitapara, Mr. Jiaqi Wu and Ms. Maleka Stewart for the insightful discussion, assistance in performing the experiments, and grant support (LLM) from National Heart, Lung, and Blood Institute (HL093708) and St. John's University.

## References

[1] D.J. Dries, Mechanical ventilation: history and harm, Air Med. J. 35 (2016) 12–15, https://doi.org/10.1016/j.amj.2015.10.006.
[2] T. Pham, L.J. Brochard, A.S. Slutsky, Mechanical ventilation: state of the art, Mayo Clin. Proc. 92 (2017) 1382–1400, https://doi.org/10.1016/j.mayocp.2017.05.004.
[3] B. Weiss, L.J. Kaplan, Oxygen therapeutics and mechanical ventilation advances, Crit. Care Clin. 33 (2017) 293–310, https://doi.org/10.1016/j.ccc.2016.12.002.
[4] A.B. Fisher, Oxygen therapy: side effects and toxicity [1, 2], Am. Rev. Respir. Dis. 122 (1980) 61–69, https://doi.org/10.1164/arrd.1980.122.5P2.61.
[5] R.H. Kallet, M.A. Matthay, Hyperoxic acute lung injury, Respir. Care 58 (2013) 123–141, https://doi.org/10.4187/respcare.01963.
[6] L.L. Mantell, S. Horowitz, J.M. Davis, J.A. Kazzaz, Hyperoxia-induced cell death in the lung-the correlation of apoptosis, necrosis, and inflammation, Ann. N. Y. Acad. Sci. 887 (1999) 171–180, https://doi.org/10.1111/j.1749-6632.1999.tb07931.x.
[7] G.L. Bassi, M. Ferrer, J.D. Marti, T. Comaru, A. Torres, Ventilator-associated pneumonia, Semin. Respir. Crit. Care Med. 35 (2014) 469–481, https://doi.org/10.1055/s-0034-1384752.
[8] J. Oliveira, C. Zagalo, P. Cavaco-Silva, Prevention of ventilator-associated pneumonia, Rev. Port. Pneumol. 20 (2014) 152–161, https://doi.org/10.1016/j.rppneu.2014.01.002.
[9] B. Allard, A. Panariti, J.G. Martin, Alveolar macrophages in the resolution of inflammation, tissue repair, and tolerance to infection, Front. Immunol. 9 (2018), https://doi.org/10.3389/fimmu.2018.01777.
[10] A.J. Byrne, S.A. Mathie, L.G. Gregory, C.M. Lloyd, Pulmonary macrophages: key players in the innate defence of the airways, Thorax 70 (2015) 1189–1196, https://doi.org/10.1136/thoraxjnl-2015-207020.
[11] A.O. Fels, Z.A. Cohn, The alveolar macrophage, J. Appl. Physiol. 60 (1986) 353–369, https://doi.org/10.1152/jappl.1986.60.2.353.
[12] F. Barbier, A. Andremont, M. Wolff, L. Bouadma, Hospital-acquired pneumonia and ventilator-associated pneumonia: recent advances in epidemiology and management, Curr. Opin. Pulm. Med. 19 (2013) 216–228, https://doi.org/10.1097/MCP.0b013e32835f27be.
[13] J. Chastre, J.-Y. Fagon, Ventilator-associated pneumonia, Am. J. Respir. Crit. Care Med. 165 (2002) 867–903, https://doi.org/10.1164/ajrccm.165.7.2105078.
[14] C.E.O. Baleeiro, S.E. Wilcoxen, S.B. Morris, T.J. Standiford, R. Paine, Sublethal hyperoxia impairs pulmonary innate immunity, J. Immunol. 171 (2003) 955–963, https://doi.org/10.4049/jimmunol.171.2.955.
[15] V.S. Patel, R.A. Sitapara, A. Gore, B. Phan, L. Sharma, V. Sampat, J.H. Li, H. Yang, S.S. Chavan, H. Wang, K.J. Tracey, L.L. Mantell, High mobility group box–1 mediates hyperoxia-induced impairment of *Pseudomonas aeruginosa* clearance and inflammatory lung injury in mice, Am. J. Respir. Cell Mol. Biol. 48 (2013) 280–287, https://doi.org/10.1165/rcmb.2012-0279OC.
[16] N.M. Reddy, S.R. Kleeberger, T.W. Kensler, M. Yamamoto, P.M. Hassoun, S. P. Reddy, Disruption of Nrf2 impairs the resolution of hyperoxia-induced acute lung injury and inflammation in mice, J. Immunol. 182 (2009) 7264, https://doi.org/10.4049/jimmunol.0804248. Baltim. Md 1950.
[17] R.A. Sitapara, A.G. Gauthier, V.S. Patel, M. Lin, M. Zur, C.R. Ashby, L.L. Mantell, GTS-21, an α7nAChR agonist, increases pulmonary bacterial clearance in mice by restoring hyperoxia-compromised macrophage function, Mol. Med. 26 (2020) 98, https://doi.org/10.1186/s10020-020-00224-9.
[18] M.A. van Zoelen, A. Ishizaka, E.K. Wolthuls, G. Choi, T. van der Poll, M.J. Schultz, Pulmonary levels of high-mobility group box 1 during mechanical ventilation and ventilator-associated pneumonia, Shock Augusta Ga 29 (2008) 441–445, https://doi.org/10.1097/SHK.0b013e318157eddd.
[19] R. Kang, R. Chen, Q. Zhang, W. Hou, S. Wu, L. Cao, J. Huang, Y. Yu, X. Fan, Z. Yan, X. Sun, H. Wang, Q. Wang, A. Tsung, T.R. Billiar, H.J. Zeh, M.T. Lotze, D. Tang, HMGB1 in health and disease, Mol. Aspect. Med. 40 (2014) 1–116, https://doi.org/10.1016/j.mam.2014.05.001.
[20] J. Wang, R. Li, Z. Peng, W. Zhou, B. Hu, X. Rao, X. Yang, J. Li, GTS-21 reduces inflammation in acute lung injury by regulating M1 polarization and function of alveolar macrophages, Shock 51 (2019) 389–400, https://doi.org/10.1097/SHK.0000000000001144.
[21] M. Entezari, D.J. Weiss, R. Sitapara, L. Whittaker, M.J. Wargo, J. Li, H. Wang, H. Yang, L. Sharma, B.D. Phan, M. Javdan, S.S. Chavan, E.J. Miller, K.J. Tracey, L. L. Mantell, Inhibition of high-mobility group box 1 protein (HMGB1) enhances bacterial clearance and protects against *Pseudomonas aeruginosa* pneumonia in cystic fibrosis, Mol. Med. 18 (2012) 477–485, https://doi.org/10.2119/molmed.2012.00024.
[22] C.A. Báez-Pagán, M. Delgado-Vélez, J.A. Lasalde-Dominicci, Activation of the macrophage α7 nicotinic acetylcholine receptor and control of inflammation, J. Neuroimmune Pharmacol. 10 (2015) 468–476, https://doi.org/10.1007/s11481-015-9601-5.
[23] D.B. Hoover, Cholinergic modulation of the immune system presents new approaches for treating inflammation, Pharmacol. Ther. 179 (2017) 1–16, https://doi.org/10.1016/j.pharmthera.2017.05.002.
[24] R.L. Papke, C. Stokes, M.I. Damaj, G.A. Thakur, K. Manther, M. Treinin, D. Bagdas, A.R. Kulkarni, N.A. Horenstein, Persistent activation of α7 nicotinic ACh receptors associated with stable induction of different desensitized states, Br. J. Pharmacol. 175 (2018) 1838–1854, https://doi.org/10.1111/bph.13851.
[25] N.A. Horenstein, R.L. Papke, A.R. Kulkarni, G.U. Chaturbhuj, C. Stokes, K. Manther, G.A. Thakur, Critical molecular determinants of α7 nicotinic acetylcholine receptor allosteric activation: separation of direct allosteric

activation and positive allosteric modulation, J. Biol. Chem. (2016), 692392, https://doi.org/10.1074/jbc.M115.692392.
[26] R.L. Papke, K. Chojnacka, N.A. Horenstein, The minimal pharmacophore for silent agonism of the α7 nicotinic acetylcholine receptor, J. Pharmacol. Exp. Therapeut. 350 (2014) 665–680, https://doi.org/10.1124/jpet.114.215236.
[27] G.A. Thakur, A.R. Kulkarni, J.R. Deschamps, R.L. Papke, Expeditious synthesis, enantiomeric resolution and enantiomer functional characterization of (4-(4-bromophenyl)-3a, 4, 5, 9b-tetrahydro-3H-cyclopenta[c]quinoline-8-sulfonamide (4BP-TQS): an allosteric agonist-positive allosteric modulator of α7 nicotinic acetylcholine receptors, J. Med. Chem. 56 (2013) 8943–8947, https://doi.org/10.1021/jm401267t.
[28] A.G. Gauthier, J. Wu, M. Lin, R. Sitapara, A. Kulkarni, G.A. Thakur, E.E. Schmidt, J.C. Perron, C.R. Ashby, L.L. Mantell, The positive allosteric modulation of alpha7-nicotinic cholinergic receptors by GAT107 increases bacterial lung clearance in hyperoxic mice by decreasing oxidative stress in macrophages, Antioxidants 10 (2021) 135, https://doi.org/10.3390/antiox10010135.
[29] B.A. Freeman, M.K. Topolosky, J.D. Crapo, Hyperoxia increases oxygen radical production in rat lung homogenates, Arch. Biochem. Biophys. 216 (1982) 477–484, https://doi.org/10.1016/0003-9861(82)90236-3.
[30] D.J. O'Donovan, C.J. Fernandes, Mitochondrial glutathione and oxidative stress: implications for pulmonary oxygen toxicity in premature infants, Mol. Genet. Metabol. 71 (2000) 352–358, https://doi.org/10.1006/mgme.2000.3063.
[31] A. Pagano, C. Barazzone-Argiroffo, Alveolar cell death in hyperoxia-induced lung injury, Ann. N. Y. Acad. Sci. 1010 (2003) 405–416, https://doi.org/10.1196/annals.1299.074.
[32] M.J. Richards, J.R. Edwards, D.H. Culver, R.P. Gaynes, Nosocomial infections in medical intensive care units in the United States. National Nosocomial Infections Surveillance System, Crit. Care Med. 27 (1999) 887–892, https://doi.org/10.1097/00003246-199905000-00020.
[33] L. Sharma, J. Wu, V. Patel, R. Sitapara, N.V. Rao, T.P. Kennedy, L.L. Mantell, Partially-desulfated heparin improves survival in *Pseudomonas* pneumonia by enhancing bacterial clearance and ameliorating lung injury, J. Immunot. 11 (2014) 260–267, https://doi.org/10.3109/1547691X.2013.839587.
[34] J. Rello, Bench-to-bedside review: therapeutic options and issues in the management of ventilator-associated bacterial pneumonia, Crit. Care 9 (2005) 259–265, https://doi.org/10.1186/cc3014.
[35] M.C. Spalding, M.W. Cripps, C.T. Minshall, Ventilator-associated pneumonia, Crit. Care Clin. 33 (2017) 277–292, https://doi.org/10.1016/j.ccc.2016.12.009.
[36] D. Bagdas, J.L. Wilkerson, A. Kulkarni, W. Toma, S. AlSharari, Z. Gul, A. H. Lichtman, R.L. Papke, G.A. Thakur, M.I. Damaj, The α7 nicotinic receptor dual allosteric agonist and positive allosteric modulator GAT107 reverses nociception in mouse models of inflammatory and neuropathic pain: α7 ago-PAM in inflammatory and neuropathic pain, Br. J. Pharmacol. 173 (2016) 2506–2520, https://doi.org/10.1111/bph.13528.
[37] M. Entezari, M. Javdan, D.J. Antoine, D.M.P. Morrow, R.A. Sitapara, V. Patel, M. Wang, L. Sharma, S. Gorasiya, M. Zur, W. Wu, J. Li, H. Yang, C.R. Ashby, D. Thomas, H. Wang, L.L. Mantell, Inhibition of extracellular HMGB1 attenuates hyperoxia-induced inflammatory acute lung injury, Redox Biol. 2 (2014) 314–322, https://doi.org/10.1016/j.redox.2014.01.013.
[38] A. Gore, A.G. Gauthier, M. Lin, V. Patel, D.D. Thomas, C.R. Ashby, L.L. Mantell, The nitric oxide donor, (Z)-1-[N-(2-aminoethyl)-N-(2-ammonioethyl)amino] diazen-1-ium-1,2-diolate (DETA-NONOate/D-NO), increases survival by attenuating hyperoxia-compromised innate immunity in bacterial clearance in a mouse model of ventilator-associated pneumonia, Biochem. Pharmacol. 176 (2020), 113817, https://doi.org/10.1016/j.bcp.2020.113817.
[39] M. Wang, S. Gorasiya, D.J. Antoine, R.A. Sitapara, W. Wu, L. Sharma, H. Yang, C. R. Ashby, D. Vasudevan, M. Zur, D.D. Thomas, L.L. Mantell, The compromise of macrophage functions by hyperoxia is attenuated by ethacrynic acid via inhibition of NF-κB–mediated release of high-mobility group box-1, Am. J. Respir. Cell Mol. Biol. 52 (2015) 171–182, https://doi.org/10.1165/rcmb.2013-0544OC.
[40] H. Wang, H. Liao, M. Ochani, M. Justiniani, X. Lin, L. Yang, Y. Al-Abed, H. Wang, C. Metz, E.J. Miller, Cholinergic agonists inhibit HMGB1 release and improve survival in experimental sepsis, Nat. Med. 10 (2004) 1216–1221.
[41] Z.-G. Luan, H. Zhang, P.-T. Yang, X.-C. Ma, C. Zhang, R.-X. Guo, HMGB1 activates nuclear factor-κB signaling by RAGE and increases the production of TNF-α in human umbilical vein endothelial cells, Immunobiology 215 (2010) 956–962, https://doi.org/10.1016/j.imbio.2009.11.001.
[42] Ma Cui, M. Beyer Andreas, Durand Matthew, V. Clough Anne, Daling Zhu, Norwood Toro Laura, Terashvili Maia, D. Ebben Johnathan, Hill R. Blake, H. Audi Said, Medhora Meetha, R. Jacobs Elizabeth, Hyperoxia causes mitochondrial fragmentation in pulmonary endothelial cells by increasing expression of pro-fission proteins, Arterioscler. Thromb. Vasc. Biol. 38 (2018) 622–635, https://doi.org/10.1161/ATVBAHA.117.310605.
[43] S. Orrenius, P. Nicotera, B. Zhivotovsky, Cell death mechanisms and their implications in toxicology, Toxicol. Sci. Off. J. Soc. Toxicol. 119 (2011) 3–19, https://doi.org/10.1093/toxsci/kfq268.
[44] D. Candas, J.J. Li, MnSOD in oxidative stress response-potential regulation via mitochondrial protein influx, Antioxidants Redox Signal. 20 (2014) 1599–1617, https://doi.org/10.1089/ars.2013.5305.
[45] M. Lin, M.T. Stewart, S. Zefi, K.V. Mateti, A. Gauthier, B. Sharma, L.R. Martinez, C.R. Ashby, L.L. Mantell, Dual effects of supplemental oxygen on pulmonary infection, inflammatory lung injury, and neuromodulation in aging and COVID-19, Free Radic. Biol. Med. 190 (2022) 247–263, https://doi.org/10.1016/j.freeradbiomed.2022.08.004.
[46] J.L. Smith, The pathological effects due to increase of oxygen tension in the air breathed, J. Physiol. 24 (1899) 19–35, https://doi.org/10.1113/jphysiol.1899.sp000746.
[47] J. Rello, D.A. Ollendorf, G. Oster, M. Vera-Llonch, L. Bellm, R. Redman, M. H. Kollef, Epidemiology and outcomes of ventilator-associated pneumonia in a large US database, Chest J 122 (2002) 2115–2121.
[48] T. Pranikoff, R.B. Hirschl, C.N. Steimle, H.L. Anderson, R.H. Bartlett, Mortality is directly related to the duration of mechanical ventilation before the initiation of extracorporeal life support for severe respiratory failure, Crit. Care Med. 25 (1997) 28–32, https://doi.org/10.1097/00003246-199701000-00008.
[49] Q. Hu, M.-H. Du, S. Hu, J. Chai, H.-M. Luo, X.-H. Hu, L. Zhang, Z.-L. Lin, L. Ma, H. Wang, Z.-Y. Sheng, PNU-282987 improves the hemodynamic parameters by alleviating vasopermeability and tissue edema in dogs subjected to a lethal burns shock, J. Burn Care Res. 35 (2014) e197, https://doi.org/10.1097/BCR.0b013e31829afe46. –e204.
[50] A.G. Gauthier, M. Lin, J. Wu, T.P. Kennedy, L.-A. Daley, C.R. Ashby, L.L. Mantell, From nicotine to the cholinergic anti-inflammatory reflex – can nicotine alleviate the dysregulated inflammation in COVID-19? J. Immunot. 18 (2021) 23–29, https://doi.org/10.1080/1547691X.2021.1875085.
[51] R.A. Sitapara, A.G. Gauthier, S.I. Valdés-Ferrer, M. Lin, V. Patel, M. Wang, A. T. Martino, J.C. Perron, C.R. Ashby, K.J. Tracey, V.A. Pavlov, L.L. Mantell, The α7 nicotinic acetylcholine receptor agonist, GTS-21, attenuates hyperoxia-induced acute inflammatory lung injury by alleviating the accumulation of HMGB1 in the airways and the circulation, Mol. Med. 26 (2020) 63, https://doi.org/10.1186/s10020-020-00177-z.
[52] K. Jaffal, S. Six, F. Zerimech, S. Nseir, Relationship between hyperoxemia and ventilator associated pneumonia, Ann. Transl. Med. (2017), https://doi.org/10.21037/atm.2017.10.15, 453–453.
[53] P. Leclerc, H. Wähämaa, H. Idborg, P.J. Jakobsson, H.E. Harris, M. Korotkova, IL-1β/HMGB1 complexes promote the PGE $_2$ biosynthesis pathway in synovial fibroblasts, Scand. J. Immunol. 77 (2013) 350–360, https://doi.org/10.1111/sji.12041.
[54] Y.-J. Lian, H. Gong, T.-Y. Wu, W.-J. Su, Y. Zhang, Y.-Y. Yang, W. Peng, T. Zhang, J.-R. Zhou, C.-L. Jiang, Y.-X. Wang, Ds-HMGB1 and fr-HMGB induce depressive behavior through neuroinflammation in contrast to nonoxid-HMGB1, Brain Behav. Immun. 59 (2017) 322–332, https://doi.org/10.1016/j.bbi.2016.09.017.
[55] F. Rocha Santos Passos, L. Heimfarth, B. Souza Monteiro, C. Bani Corrêa, T. Rodrigues de Moura, A. Antunes de Souza Araújo, P. Ricardo Martins-Filho, L. J. Quintans-Júnior, J. de Souza Siqueira Quintans, Oxidative stress and inflammatory markers in patients with COVID-19: potential role of RAGE, HMGB1, GFAP and COX-2 in disease severity, Int. Immunopharm. 104 (2022), 108502, https://doi.org/10.1016/j.intimp.2021.108502.
[56] H. Wang, O. Bloom, M. Zhang, J.M. Vishnubhakat, M. Ombrellino, J. Che, A. Frazier, H. Yang, S. Ivanova, L. Borovikova, K.R. Manogue, E. Faist, E. Abraham, J. Andersson, U. Andersson, P.E. Molina, N.N. Abumrad, A. Sama, K. J. Tracey, HMG-1 as a late mediator of endotoxin lethality in mice, Science 285 (1999) 248–251.
[57] U. Andersson, K.J. Tracey, H. Yang, Post-translational modification of HMGB1 disulfide bonds in stimulating and inhibiting inflammation, Cells 10 (2021) 3323, https://doi.org/10.3390/cells10123323.
[58] R. Chen, R. Kang, D. Tang, The mechanism of HMGB1 secretion and release, Exp. Mol. Med. 54 (2022) 91–102, https://doi.org/10.1038/s12276-022-00736-w.
[59] L. Pellegrini, E. Foglio, E. Pontemezzo, A. Germani, M.A. Russo, F. Limana, HMGB1 and repair: focus on the heart, Pharmacol. Ther. 196 (2019) 160–182, https://doi.org/10.1016/j.pharmthera.2018.12.005.
[60] The NU SCRIPT Study Investigators, R.A. Grant, L. Morales-Nebreda, N. S. Markov, S. Swaminathan, M. Querrey, E.R. Guzman, D.A. Abbott, H. K. Donnelly, A. Donayre, I.A. Goldberg, Z.M. Klug, N. Borkowski, Z. Lu, H. Kihshen, Y. Politanska, L. Sichizya, M. Kang, A. Shilatifard, C. Qi, J. W. Lomasney, A.C. Argento, J.M. Kruser, E.S. Malsin, C.O. Pickens, S.B. Smith, J. M. Walter, A.E. Pawlowski, D. Schneider, P. Nannapaneni, H. Abdala-Valencia, A. Bharat, C.J. Gottardi, G.R.S. Budinger, A.V. Misharin, B.D. Singer, R. G. Wunderink, Circuits between infected macrophages and T cells in SARS-CoV-2 pneumonia, Nature 590 (2021) 635–641, https://doi.org/10.1038/s41586-020-03148-w.
[61] U. Andersson, H. Wang, K. Palmblad, A.-C. Aveberger, O. Bloom, H. Erlandsson-Harris, A. Janson, R. Kokkola, M. Zhang, H. Yang, K.J. Tracey, High mobility group 1 protein (Hmg-1) stimulates proinflammatory cytokine synthesis in human monocytes, J. Exp. Med. 192 (2000) 565–570, https://doi.org/10.1084/jem.192.4.565.
[62] Q. Gao, S. Wang, X. Chen, S. Cheng, Z. Zhang, F. Li, L. Huang, Y. Yang, B. Zhou, D. Yue, D. Wang, L. Cao, N.R. Maimela, B. Zhang, J. Yu, L. Wang, Y. Zhang, Cancer-cell-secreted CXCL11 promoted CD8+ T cells infiltration through docetaxel-induced-release of HMGB1 in NSCLC, J. Immunother. Cancer 7 (2019) 42, https://doi.org/10.1186/s40425-019-0511-6.
[63] M. Wang, A. Gauthier, L. Daley, K. Dial, J. Wu, J. Woo, M. Lin, C. Ashby, L. L. Mantell, The role of HMGB1, a nuclear damage-associated molecular pattern molecule, in the pathogenesis of lung diseases, Antioxidants Redox Signal. 31 (2019) 954–993, https://doi.org/10.1089/ars.2019.7818.
[64] H. Yang, H. Wang, U. Andersson, Targeting inflammation driven by HMGB1, Front. Immunol. 11 (2020) 484, https://doi.org/10.3389/fimmu.2020.00484.
[65] H. Yang, H. Liu, Q. Zeng, G.H. Imperato, M.E. Addorisio, J. Li, M. He, K.F. Cheng, Y. Al-Abed, H.E. Harris, S.S. Chavan, U. Andersson, K.J. Tracey, Inhibition of HMGB1/RAGE-mediated endocytosis by HMGB1 antagonist box A, anti-HMGB1 antibodies, and cholinergic agonists suppresses inflammation, Mol. Med. 25 (2019) 13, https://doi.org/10.1186/s10020-019-0081-6.

[66] U. Andersson, W. Ottestad, K.J. Tracey, Extracellular HMGB1: a therapeutic target in severe pulmonary inflammation including COVID-19? Mol. Med. 26 (2020) 42, https://doi.org/10.1186/s10020-020-00172-4.
[67] M.C. Maldifassi, G. Atienza, F. Arnalich, E. López-Collazo, J.L. Cedillo, C. Martín-Sánchez, A. Bordas, J. Renart, C. Montiel, A new IRAK-M-mediated mechanism implicated in the anti-inflammatory effect of nicotine via α7 nicotinic receptors in human macrophages, PLoS One 9 (2014), e108397, https://doi.org/10.1371/journal.pone.0108397.
[68] R. Malaviya, J.D. Laskin, D.L. Laskin, Anti-TNFα therapy in inflammatory lung diseases, Pharmacol. Ther. 180 (2017) 90–98, https://doi.org/10.1016/j.pharmthera.2017.06.008.
[69] S. Mukhopadhyay, J.R. Hoidal, T.K. Mukherjee, Role of TNFα in pulmonary pathophysiology, Respir. Res. 7 (2006) 125, https://doi.org/10.1186/1465-9921-7-125.
[70] J.M. Swanson, E.W. Mueller, M.A. Croce, G.C. Wood, B.A. Boucher, L.J. Magnotti, T.C. Fabian, Changes in pulmonary cytokines during antibiotic therapy for ventilator-associated pneumonia, Surg. Infect. 11 (2010) 161–167, https://doi.org/10.1089/sur.2008.067.
[71] L.L. Mantell, W.R. Parrish, L. Ulloa, HMGB-1 as a therapeutic target for infectious and inflammatory disorders, Shock 25 (2006) 4–11, https://doi.org/10.1097/01.shk.0000188710.04777.9e.
[72] R. Rafikov, V. Nair, S. Sinari, H. Babu, J.C. Sullivan, J.X.-J. Yuan, A.A. Desai, O. Rafikova, Gender difference in damage-mediated signaling contributes to pulmonary arterial hypertension, Antioxidants Redox Signal. 31 (2019) 917–932, https://doi.org/10.1089/ars.2018.7664.
[73] M. Zemskova, S. Kurdyukov, J. James, N. McClain, R. Rafikov, O. Rafikova, Sex-specific stress response and HMGB1 release in pulmonary endothelial cells, PLoS One 15 (2020), e0231267, https://doi.org/10.1371/journal.pone.0231267.
[74] B. Lu, K. Kwan, Y.A. Levine, P.S. Olofsson, H. Yang, J. Li, S. Joshi, H. Wang, U. Andersson, S.S. Chavan, K.J. Tracey, α7 nicotinic acetylcholine receptor signaling inhibits inflammasome activation by preventing mitochondrial DNA release, Mol. Med. 20 (2014) 350–358, https://doi.org/10.2119/molmed.2013.00117.
[75] E. Bancalari, N. Claure, D. Jain, Neonatal respiratory therapy, in: Avery's Diseases of the Newborn, Elsevier, 2018, pp. 632–652.e6, https://doi.org/10.1016/B978-0-323-40139-5.00045-0.
[76] F. He, Q. Wu, B. Xu, X. Wang, J. Wu, L. Huang, J. Cheng, Suppression of Stim1 reduced intracellular calcium concentration and attenuated hypoxia/reoxygenation induced apoptosis in H9C2 cells, Biosci. Rep. 37 (2017), BSR20171249, https://doi.org/10.1042/BSR20171249.
[77] S. Orrenius, V. Gogvadze, B. Zhivotovsky, Mitochondrial oxidative stress: implications for cell death, Annu. Rev. Pharmacol. Toxicol. 47 (2007) 143–183, https://doi.org/10.1146/annurev.pharmtox.47.120505.105122.
[78] A.A. Starkov, The role of mitochondria in reactive oxygen species metabolism and signaling, Ann. N. Y. Acad. Sci. 1147 (2008) 37–52, https://doi.org/10.1196/annals.1427.015.
[79] N. Suematsu, H. Tsutsui, J. Wen, D. Kang, M. Ikeuchi, T. Ide, S. Hayashidani, T. Shiomi, T. Kubota, N. Hamasaki, A. Takeshita, Oxidative stress mediates tumor necrosis factor-α–induced mitochondrial DNA damage and dysfunction in cardiac myocytes, Circulation 107 (2003) 1418–1423, https://doi.org/10.1161/01.CIR.0000055318.09997.1F.
[80] D.L. Hoffman, P.S. Brookes, Oxygen sensitivity of mitochondrial reactive oxygen species generation depends on metabolic conditions, J. Biol. Chem. 284 (2009) 16236–16245, https://doi.org/10.1074/jbc.M809512200.
[81] V. Ratner, A. Starkov, D. Matsiukevich, R.A. Polin, V.S. Ten, Mitochondrial dysfunction contributes to alveolar developmental arrest in hyperoxia-exposed mice, Am. J. Respir. Cell Mol. Biol. 40 (2009) 511–518, https://doi.org/10.1165/rcmb.2008-0341RC.
[82] O. Ozden, S.-H. Park, H.-S. Kim, H. Jiang, M.C. Coleman, D.R. Spitz, D. Gius, Acetylation of MnSOD directs enzymatic activity responding to cellular nutrient status or oxidative stress, Aging 3 (2011) 102–107.
[83] Y. Wang, R. Branicky, A. Noë, S. Hekimi, Superoxide dismutases: dual roles in controlling ROS damage and regulating ROS signaling, J. Cell Biol. 217 (2018) 1915–1928, https://doi.org/10.1083/jcb.201708007.
[84] K. Kokubo, S. Soeda, T. Shinbo, M. Hirose, N. Fuku, Y. Nishigaki, M. Tanaka, H. Kobayashi, Macrophages that survive hyperoxia exposure have higher superoxide dismutase activities in their mitochondria, Adv. Exp. Med. Biol. 662 (2010) 63–69, https://doi.org/10.1007/978-1-4419-1241-1_8.
[85] C. Aerts, B. Wallaert, P. Gosset, C. Voisin, Relationship between oxygen-induced alveolar macrophage injury and cell antioxidant defence, J. Appl. Toxicol. 15 (1995) 53–58, https://doi.org/10.1002/jat.2550150112.
[86] Y. Arita, J.A. Kazzaz, A. Joseph, H. Koo, Y. Li, J.M. Davis, Antioxidants improve antibacterial function in hyperoxia-exposed macrophages, Free Radic. Biol. Med. 42 (2007) 1517–1523, https://doi.org/10.1016/j.freeradbiomed.2007.02.003.
[87] D.M.P. Morrow, T. Entezari-Zaherab, J. Romashko, A.O. Azghani, M. Javdan, L. Ulloa, E.J. Miller, L.L. Mantell, Antioxidants preserve macrophage phagocytosis of *Pseudomonas aeruginosa* during hyperoxia, Free Radic. Biol. Med. 42 (2007) 1338–1349, https://doi.org/10.1016/j.freeradbiomed.2007.01.031.
[88] Y.S. Ho, M.S. Dey, J.D. Crapo, Antioxidant enzyme expression in rat lungs during hyperoxia, Am. J. Physiol. 270 (1996) L810–L818, https://doi.org/10.1152/ajplung.1996.270.5.L810.
[89] V. Demicheli, D.M. Moreno, R. Radi, Human Mn-superoxide dismutase inactivation by peroxynitrite: a paradigm of metal-catalyzed tyrosine nitration in vitro and in vivo, Metallomics 10 (2018) 679–695, https://doi.org/10.1039/C7MT00348J.
[90] A.E. Dikalova, H.A. Itani, R.R. Nazarewicz, W.G. McMaster, C.R. Flynn, R. Uzhachenko, J.P. Fessel, J.L. Gamboa, D.G. Harrison, S.I. Dikalov, Sirt3 impairment and SOD2 hyperacetylation in vascular oxidative stress and hypertension, Circ. Res. 121 (2017) 564–574, https://doi.org/10.1161/CIRCRESAHA.117.310933.
[91] Y.S. Kim, P. Gupta Vallur, R. Phaëton, K. Mythreye, N. Hempel, Insights into the dichotomous regulation of SOD2 in cancer, Antioxidants 6 (2017), https://doi.org/10.3390/antiox6040086.
[92] N.K. Patil, H. Saba, L.A. MacMillan-Crow, Effect of S-nitrosoglutathione on renal mitochondrial function: a new mechanism for reversible regulation of manganese superoxide dismutase activity? Free Radic. Biol. Med. 56 (2013) 54–63, https://doi.org/10.1016/j.freeradbiomed.2012.12.001.
[93] F. Yamakura, H. Kawasaki, Post-translational modifications of superoxide dismutase, Biochim. Biophys. Acta BBA - Proteins Proteomics, Carbonic Anhydrase and Superoxide Dismutase 1804 (2010) 318–325, https://doi.org/10.1016/j.bbapap.2009.10.010.
[94] Y.M.W. Janssen-Heininger, J.D. Nolin, S.M. Hoffman, J.L. van der Velden, J. E. Tully, K.G. Lahue, S.T. Abdalla, D.G. Chapman, N.L. Reynaert, A. van der Vliet, V. Anathy, Emerging mechanisms of glutathione-dependent chemistry in biology and disease, J. Cell. Biochem. 114 (2013), https://doi.org/10.1002/jcb.24551.
[95] W. Zhou, X. Yuan, L. Zhang, B. Su, D. Tian, Y. Li, J. Zhao, Y. Wang, S. Peng, Overexpression of HO-1 assisted PM2.5-induced apoptosis failure and autophagy-related cell necrosis, Ecotoxicol. Environ. Saf. 145 (2017) 605–614, https://doi.org/10.1016/j.ecoenv.2017.07.047.
[96] H. Patel, J. McIntire, S. Ryan, A. Dunah, R. Loring, Anti-inflammatory effects of astroglial α7 nicotinic acetylcholine receptors are mediated by inhibition of the NF-κB pathway and activation of the Nrf2 pathway, J. Neuroinflammation 14 (2017), https://doi.org/10.1186/s12974-017-0967-6.
[97] K. Tsoyi, H.J. Jang, J.W. Kim, H.K. Chang, Y.S. Lee, H.-O. Pae, H.J. Kim, H.G. Seo, J.H. Lee, H.-T. Chung, K.C. Chang, Stimulation of Alpha7 nicotinic acetylcholine receptor by nicotine attenuates inflammatory response in macrophages and improves survival in experimental model of sepsis through heme oxygenase-1 induction, Antioxidants Redox Signal. 14 (2011) 2057–2070, https://doi.org/10.1089/ars.2010.3555.
[98] Q. Zhang, Y. Lai, J. Deng, Menglong Wang, Z. Wang, Meng Wang, Y. Zhang, X. Yang, X. Zhou, H. Jiang, Vagus nerve stimulation attenuates hepatic ischemia/reperfusion injury via the Nrf2/HO-1 pathway, Oxid. Med. Cell. Longev 2019 (2019) 1–10, https://doi.org/10.1155/2019/9549506.
[99] T.R. Hurd, N.J. Costa, C.C. Dahm, S.M. Beer, S.E. Brown, A. Filipovska, M. P. Murphy, Glutathionylation of mitochondrial proteins, Antioxidants Redox Signal. 7 (2005) 999–1010, https://doi.org/10.1089/ars.2005.7.999.
[100] V.J. Findlay, D.M. Townsend, T.E. Morris, J.P. Fraser, L. He, K.D. Tew, A novel role for human sulfiredoxin in the reversal of glutathionylation, Cancer Res. 66 (2006) 6800–6806, https://doi.org/10.1158/0008-5472.CAN-06-0484.
[101] Y. Janssen-Heininger, N.L. Reynaert, A. van der Vliet, V. Anathy, Endoplasmic reticulum stress and glutathione therapeutics in chronic lung diseases, Redox Biol. 33 (2020), 101516, https://doi.org/10.1016/j.redox.2020.101516.